NASA TECHNICAL NOTE

NASA TN D-2448

c. /

NASA TN D-2448

ACCURACY OF NAVIGATION IN VARIOUS REGIONS OF EARTH-MOON SPACE WITH VARIOUS COMBINATIONS OF ONBOARD OPTICAL MEASUREMENTS

by Alton P. Mayo, Ruben L. Jones, and William M. Adams

*Langley Research Center
Langley Station, Hampton, Va.*

NATIONAL AERONAUTICS AND SPACE ADMINISTRATION • WASHINGTON, D. C. • SEPTEMBER 1964

ACCURACY OF NAVIGATION IN VARIOUS REGIONS OF EARTH-MOON SPACE WITH VARIOUS COMBINATIONS OF ONBOARD OPTICAL MEASUREMENTS

By Alton P. Mayo, Ruben L. Jones, and William M. Adams

Langley Research Center
Langley Station, Hampton, Va.

NATIONAL AERONAUTICS AND SPACE ADMINISTRATION

For sale by the Office of Technical Services, Department of Commerce,
Washington, D.C. 20230 -- Price $1.25

ACCURACY OF NAVIGATION IN VARIOUS REGIONS OF EARTH-MOON SPACE WITH VARIOUS COMBINATIONS OF ONBOARD OPTICAL MEASUREMENTS

By Alton P. Mayo, Ruben L. Jones, and William M. Adams
Langley Research Center

SUMMARY

A study was made of the relative accuracies of 60 combinations of onboard optical observations that may be available for use in determining the position and velocity of a spacecraft from the vicinity of the earth to the vicinity of the moon. The method of analysis consisted of computing along a nominal trajectory the mathematically correct onboard-optical-observation angles for specified times, adding random errors to the optical observations, computing transition matrices, and statistically reducing the results to obtain the estimated errors in the initial position and velocity for a particular region of the trajectory.

The procedure used is discussed and the method of computation is given. Data presented show the effects of the number of observations and the frequency of observation on the accuracy of determining position and velocity. Accuracies for some of the better combinations of measurements studied are plotted over the earth-moon region.

The study indicated that the estimated errors in position and velocity of the spacecraft tend to converge after 40 observations when the observations were made at a rate of 10 per hour. On the basis of these results, errors in position and velocity for various combinations of optical observations were computed and compared. The errors are given as root-sum-square values of the estimates and standard deviations. The results revealed that, for an assumed standard deviation in instrument error of 10 arc-seconds (except for horizon-type measurements near the earth or moon), the better of the combinations of observations studied were as follows: (a) Near the earth, the combination of optical measurements of the earth's angular diameter, azimuth, and elevation, or equivalently angular diameter and two stars to body center, was most accurate. The contribution of angular diameter to the accuracy in this region was, however, small and the use of only azimuth and elevation or two stars to body center gave approximately the same results. (b) For the regions beginning 1.5 hours after insertion (a radial distance from earth's center to spacecraft of 31,704 km), the most accurate combination consisted of the onboard observation of the angles between the earth's horizon and three stars as seen from the spacecraft. (c) For the remainder of the trajectory up to the moon's sphere of influence, the most accurate combination consisted of the measurement of the

angle between the horizon of the earth and one star and the angles between the horizon of the moon and two stars.

In the terminal region within the moon's sphere of influence, measurements made solely on the moon would be expected to be of the highest accuracy. Results are not presented for this region; however, the results should be somewhat similar to those obtained by using measurements made on the earth at close range.

INTRODUCTION

Two approaches have been proposed for achieving the goal of midcourse circumlunar navigation - that is, for determining the position and velocity of a spacecraft in earth-moon space. One method employs earth-based radio measurements (ref. 1) and the other utilizes onboard optical measurements (refs. 2 and 3). The optical method which has been given much attention lately is the technique investigated in this study.

Briefly, the procedure of optical midcourse navigation involves taking many optical measurements over an interval of time and transitioning the data to obtain equivalent data for a future specified time. After these data are statistically reduced to obtain the best estimate of the spacecraft's position and velocity vectors at that time, the necessary corrections to the trajectory may be computed. This procedure may be repeated for various regions of the trajectory.

Many types of optical navigational sightings may be made in the various regions of earth-moon space (ref. 4); however, in certain regions some combinations are more accurate than others (for example, see refs. 5 and 6). For this reason the onboard navigation system should select the most effective measurements for a particular region.

In the present paper, many different combinations of optical measurements that may be available for determining the spacecraft's position and velocity are studied. The theory of the navigation procedure used is discussed and the methods employed are given. Accuracies of a large number of the combinations in the various regions are presented in tabular form for comparison purposes. Although some of the combinations chosen were expected to be less accurate than others, they were also included to show the size of errors. Moreover, there may be omissions of combinations of greater accuracy than those presented. Data presented establish the position and velocity accuracies for a given number of position fixes (combinations of two or three observations) and rate of observation. Accuracies for the better combinations of measurements studied are plotted over the earth-moon region.

SYMBOLS

a,b,c	direction cosine of line of sight to star with respect to X-, Y-, Z-axis, respectively; subscripts 1, 2, and 3 are used to refer to particular stars (see table I)
G	uncertainty in determining horizon
i	orbital inclination of beacon
K	a particular set of earth and moon referenced observations
M	matrix of partial derivatives of angular measurements with respect to trajectory variables
m	onboard optical measurement; subscript 1, 2, or 3 is used to refer to a particular onboard type of measurement
Δm	random error in measurement
n	number of space angles observed
Q	element of matrix $\left\{\left\|M\right\|_{to,t}^{T*}\left\{\Delta M\right\}_{t}^{*}\right\}$
q	element of matrix $\left[\left\|M\right\|_{to,t}^{T*}\left\|M\right\|_{to,t}^{*}\right]$
R	radius of earth or moon
R_B	radial distance from earth's or moon's center to beacon
r	radial distance from body's center to vehicle
t	time from beginning of region of observation
W	weight given to one observation
X,Y,Z	earth-centered, inertial, rectangular coordinate axes
x,y,z	orthogonal components of earth-centered, inertial, right-hand, rectangular coordinate system
x_1,y_1,z_1	coordinates for trajectory 1 in x, y, z directions
x_2,y_2,z_2	coordinates for trajectory 2 in x, y, z directions

$\Delta x, \Delta y, \Delta z$	incremental change or estimate of error in x-, y-, z-component of trajectory, respectively
$\widehat{\Delta x}, \widehat{\Delta y}, \widehat{\Delta z}$	incremental change in x-, y-, z-component, respectively, of landmark or beacon
Δr	root sum square of best estimate of error in position, $\left(\Delta x^2 + \Delta y^2 + \Delta z^2\right)^{1/2}$
Δv	root sum square of best estimate of error in velocity, $\left(\Delta \dot{x}^2 + \Delta \dot{y}^2 + \Delta \dot{z}^2\right)^{1/2}$
α	subtended angle (vehicle-centered inertial coordinate system)
δM	matrix of deviations in angular measurements resulting from a departure from reference trajectory
δm	deviation in a single angular observation
ΔM	matrix of deviations in actual onboard measurements
δX	matrix of deviations of position and velocity in x, y, z directions
ΔX	matrix of most probable errors in position and velocity in x, y, z directions
$\delta x, \delta y, \delta z$	deviation in x-, y-, z-component, respectively
ϵ	matrix of errors in measurements
λ	longitude of landmark or beacon on earth or moon at t_o
σ	standard deviation
σ_I	standard deviation of range independent component of the random error
σ_r	root sum square of standard deviations of error in position, $\left(\sigma_x{}^2 + \sigma_y{}^2 + \sigma_z{}^2\right)^{1/2}$
σ_v	root sum square of standard deviations of error in velocity, $\left(\sigma_{\dot{x}}{}^2 + \sigma_{\dot{y}}{}^2 + \sigma_{\dot{z}}{}^2\right)^{1/2}$
ϕ	geocentric latitude of landmark or beacon for earth or moon at t_o
ω	angular velocity of earth, moon, or orbiting beacon

Subscripts:

B	orbiting beacon of earth or moon
E	earth referenced observation
e	earth center
i	particular angular observation
j	particular column of a matrix
L	landmark on earth or moon
M	moon referenced observation
m	moon center
o	initial point
t	time of particular observation i
t_o	initial time of observation
s	a particular row of a matrix
meas	measured

Notation:

$[\;]$	square matrix
$\|\|\;\|\|$	rectangular matrix
$\{\;\}$	column matrix
$\|\;\|$	absolute value

Matrix exponents:

T	indicates the transpose
-1	indicates the inverse
*	indicates a weighted quantity

Bar over symbol indicates a vector. Variables separated by commas and in parentheses are vectors.

Two vectors separated by a dot denote a dot product.

A derivative with respect to time is denoted by a dot over the variable - for example, $dx/dt = \dot{x}$.

NAVIGATION MEASUREMENTS

The accuracies of various combinations of optical observations available for midcourse earth-moon navigation are compared in this study. To establish the accuracies obtainable from a given number of observations and rate of observation, cases were investigated in which (1) the rate of observation was maintained constant and (2) the number of observations was maintained constant. The onboard optical observations assumed available were:

Subtended angle of the earth

Subtended angle of the moon

Angle between the earth's horizon and a star

Angle between the moon's horizon and a star

Angle between the earth's center and a star

Angle between the moon's center and a star

Angle between an orbiting earth beacon and a star

Angle between an orbiting moon beacon and a star

Angle between an earth landmark and a star

Angle between a moon landmark and a star

Azimuth of the earth as measured in vehicle-centered coordinate system

Azimuth of the moon as measured in vehicle-centered coordinate system

Elevation of the earth as measured in vehicle-centered coordinate system

The positions of three stars of the first magnitude, selected for this study, are given in table I. The directions of these stars form an orthogonal axis system with the stars approximately 20°, 40°, and 60° to the orbital plane. This orientation is desirable for accuracy considerations since the star-to-body angles are sensitive to vehicle motions both in the nominal trajectory plane and perpendicular to it.

The landmarks used were chosen in the respective equatorial planes of the earth and the moon and were assumed to lie on the positive X-axis at the beginning of each region. In the sighting in which the moon landmark and beacon were used, a moon-centered, right-hand, inertial coordinate system was assumed with the respective axes parallel to the earth-centered axes. Furthermore, for simplicity, the moon's spin axis was assumed to be parallel to that of the earth. The earth beacon and the moon beacon were assumed to be in circular orbits of 5,000-mile radii and the inclination of each orbit was taken to be 50° with the ascending node on the X-axis. Under these conditions the landmarks and beacons will not always be visible; however, for this study it was adequate to assume them to be mathematically visible at all times.

The various optical observations were assumed to be weighted according to the equation $W = 1/\sigma$, where σ is the standard deviation of the corresponding measurement error.

Inasmuch as the effectiveness of a particular combination of measurements is expected to vary for different regions of earth-moon space, each measuring combination was investigated in six regions as illustrated in figure 1. (The first and second regions overlap.) In each region, combinations of measurements were made and for the main part of the study these measurements were assumed to be taken for 4 hours at a rate of 10 per hour (one position fix consists of two to three simultaneous measurements). In reality, for a position fix the measurements would not be made simultaneously; however, this restriction does not alter the results of the present study. It was assumed that the trajectory would be redetermined for each region and that the position fixes were equally spaced in time. Thus, the position and velocity results for a particular region are independent of measurements made in other regions. In an actual mission the measurements made in a given region would probably be governed by overall accuracy considerations of the entire flight.

A block diagram of the computational program used in this study is given in figure 2. Six possible sets ($K = 0$ to $K = 5$) of optical observations are available. In each set, three types of measurements may be made on the earth and the same three may be made on the moon. Of the many available combinations of earth and moon referenced observations, 10 combinations were selected in each set to be evaluated in each of 6 regions of space. (See table II.) Thus, for this study, 360 combinations were analyzed over the earth-moon region. As a consequence, a shorthand method was devised to represent each case. A three-digit number was used for this purpose; for example, consider case 410. The first digit of case 410 refers to the observation time of 4 hours; the second digit refers to the set of observations corresponding to the value of $K = 1$ in the block diagram of figure 2; the third digit refers to the particular combination of the six optical observations available in the set for $K = 1$. In table II a list is given of the selected combinations of optical observations which correspond to the third digit.

In order to facilitate the tabular description of the types of observations for each case, a set of astronomical symbols was devised. These symbols are defined as follows:

 subtended angle of the earth

☽▷	subtended angle of the moon
$\bar{\bigcirc}$	observation to the earth's horizon
$\bar{☽}$	observation to the moon's horizon
⊕	observation to the earth's center
+☽	observation to the moon's center
$\ast_1, \ast_2, \ast_3$	observation to star 1, star 2, and star 3, respectively
⊘	observation of an orbiting earth beacon
⊘☽	observation of an orbiting moon beacon
Ⓛ	observation of an earth landmark
L☽	observation of a moon landmark
Ⓐ	observation of the earth's azimuth
Ⓔ	observation of the earth's elevation
A☽	observation of the moon's azimuth
E☽	observation of the moon's elevation

The symbols are combined in the appropriate order to describe any particular combination. For example, the combination composed of the angles of the subtended angle of the earth, of the angle included by star 1, the vehicle, and the moon's horizon, of the angle included by star 2, the vehicle, and the moon's horizon for a 4-hour interval of time is case 407 and may be written with the aid of the astronomical symbols as ○▷, $\ast_1$☽, $\ast_2$☽.

The 4-hour cases for each region and a description of the corresponding optical angles are given in tables III to VIII.

The computing time required to calculate a 4-hour segment of the trajectory and the 60 cases by an electronic data processing system was approximately 1 hour, and because of the time required it was decided to analyze a typical set of instrument errors only (i.e., only one value of σ).

THEORY AND COMPUTATIONAL TECHNIQUE

For this study, a right-hand inertial Cartesian coordinate system was chosen. The origin is defined to be at the earth's center except when it was required to have origins at the moon's center (calculations pertaining to moon landmark or orbiting beacon) or at the vehicle's center (for calculating space angles); for these observations the axes are assumed to be parallel to those of the earth-centered system. The X-axis is positive in the direction of the mean equinox at midnight of December 31, 1967 and lies in or parallel to the equatorial plane. The Z-axis lies along or parallel to the spin axis of the earth and is positive in the positive direction of spin. The Y-axis is normal to the XZ-plane and completes the right-hand system. (See ref. 7 for a further description of the coordinate system and the trajectory computational technique.)

Theory

If deviations in position and velocity at some existing time after insertion, t_o hours, are assumed to be linearly related to those resulting at some future time after insertion, t hours, then the deviations at time t are related to the values at time t_o by

$$\begin{Bmatrix} \delta x \\ \delta y \\ \delta z \\ \delta \dot{x} \\ \delta \dot{y} \\ \delta \dot{z} \end{Bmatrix}_t = \left[\Phi\right]_{to,t} \begin{Bmatrix} \delta x \\ \delta y \\ \delta z \\ \delta \dot{x} \\ \delta \dot{y} \\ \delta \dot{z} \end{Bmatrix}_{to} \tag{1}$$

where $\left[\Phi\right]_{to,t}$ is a square matrix (transition matrix) of 36 partial derivatives of each of the trajectory variables x_t, y_t, z_t, $\dot{x}_t$, $\dot{y}_t$, and $\dot{z}_t$ with respect to each of the variables x_{to}, y_{to}, z_{to}, $\dot{x}_{to}$, $\dot{y}_{to}$, and $\dot{z}_{to}$, and

$$\begin{Bmatrix} \delta x \\ \delta y \\ \delta z \\ \delta \dot{x} \\ \delta \dot{y} \\ \delta \dot{z} \end{Bmatrix}_t \quad \text{and} \quad \begin{Bmatrix} \delta x \\ \delta y \\ \delta z \\ \delta \dot{x} \\ \delta \dot{y} \\ \delta \dot{z} \end{Bmatrix}_{to}$$

are the column matrices of the future deviations and of the existing deviations in position and velocity, respectively. In shorter form, equation (1) becomes

$$\left\{\delta X\right\}_t = \left[\Phi\right]_{to,t} \left\{\delta X\right\}_{to} \tag{2}$$

For the sighting in which optical measurements m_i are made (where the subscript i indicates a particular angular measurement - that is, subtended angle, azimuth, etc.), the deviations resulting from a departure from the reference trajectory at t hours are related to those at t_o hours by

$$\delta m_{i,t} = \frac{\partial m_{i,t}}{\partial x_{to}} \delta x_{to} + \frac{\partial m_{i,t}}{\partial y_{to}} \delta y_{to} + \frac{\partial m_{i,t}}{\partial z_{to}} \delta z_{to} + \frac{\partial m_{i,t}}{\partial \dot{x}_{to}} \delta \dot{x}_{to}$$

$$+ \frac{\partial m_{i,t}}{\partial \dot{y}_{to}} \delta \dot{y}_{to} + \frac{\partial m_{i,t}}{\partial \dot{z}_{to}} \delta \dot{z}_{to}$$

where the partial derivatives of the measurement with respect to the individual components of initial velocity and initial position are assumed to vary linearly with respect to the trajectory variables. Thus,

$$\left\{\delta M\right\}_t = \left\|M\right\|_{to,t} \left\{\delta X\right\}_{to} \tag{3}$$

where $\left\{\delta M\right\}_t$ is the column matrix of the measured deviations in the angle m_1, m_2, and m_3 referenced to the earth and moon and $\left\|M\right\|_{to,t}$ is the rectangular (n by 6) matrix of the partial derivatives of the measurements with respect to the trajectory variables.

It will be assumed that the navigation system will make n optical observations at a known rate for each region. Because of instrument errors, and so forth, the observations will be in error. Equation (3) implies that each observation has zero error. Therefore, the matrix equation relating the observations to the unknowns becomes

$$\{\Delta M\}_t = \|M\|_{to,t} \{\delta X\}_{to} + \{\epsilon\}_t \tag{4}$$

If the matrix of errors $\{\epsilon\}_t$ is assumed to be random with Gaussian distributions having a zero mean and a variance of σ^2, and not being correlated, the most probable value of the unknowns $\left(\text{denoted by } \{\Delta X\}_{to}\right)$ is obtained by weighting each of the n observation equations by multiplying by the reciprocal of the corresponding standard deviation σ of the measurement error and solving the resulting system for those unknowns which minimize the sum of the squares of the weighted residuals. If the weighted observations are denoted by $\{\Delta M\}_t^*$ and the weighted observation coefficients by $\|M\|_{to,t}^*$, the most probable value of $\{\delta X\}_{to}$ $\left(\text{denoted by } \{\Delta X\}_{to}\right)$ is (according to ref. 8):

$$\{\Delta X\}_{to} = \left[\|M\|_{to,t}^{T*}\|M\|_{to,t}^{*}\right]^{-1} \|M\|_{to,t}^{T*} \{\Delta M\}_t^* \tag{5}$$

Besides the inherent inaccuracy of the instrument, those measurements which involve the observation of a single horizon have an additional instrument error due to the horizon uncertainty. The standard deviation of the total error in a horizon measurement is expressed as

$$\sigma_i = \sqrt{\sigma_I{}^2 + \frac{G^2}{r^2 - R^2}} \tag{6}$$

where σ_I represents the instrument error, G^2 represents the variance σ^2 of the error due to horizon uncertainty, r is the distance from the vehicle to the body's center, and R is the mean radius of the body.

Computational Technique

The reference trajectory utilized for this study is a fairly low-energy earth-moon trajectory such as would be used for a circumlunar trip or a lunar landing. The assumed launch date is March 18, 1968, and the time of closest passage to the moon is about 70.6 hours from earth injection. The spacecraft trajectory was generated by using a seven-body (earth, moon, Jupiter, Venus, Mars, sun, spacecraft) trajectory computational program based on Encke's perturbation technique. (See ref. 7 for details of the program and ref. 9 for details of the trajectory.) A three-dimensional plot of the reference trajectory is shown in figure 1.

Eight trajectories and the optical-measurement angles at the respective time points were computed in accordance with the block diagram of figure 2 (see the appendix for the equations for the angles corresponding to the various optical observations); trajectory 8 is assumed to be the actual trajectory traversed by the spacecraft and trajectory 1 is the nominal or reference trajectory. The remaining six are the disturbed trajectories (a trajectory that differs from the reference trajectory by a small increment in one of its parameters) used to compute the partial derivatives in the matrices $[\Phi]_{to,t}$ and $\|M\|_{to,t}$.

For the method chosen to compute the elements of $[\Phi]_{to,t}$ and $\|M\|_{to,t}$, the assumption is made that the disturbances are sufficiently small to allow, for example, the approximation

$$\frac{\partial x_t}{\partial x_{to}} \approx \frac{(x_t)_{disturbed} - (x_t)_{nominal}}{\Delta x_{to}}$$

Thus, subtracting the parameters of trajectory 1 from those of trajectory 2 and dividing the result by Δx_{to} yields $\partial x_t/\partial x_{to}$, $\partial y_t/\partial x_{to}$, $\partial z_t/\partial x_{to}$, $\partial \dot{x}_t/\partial x_{to}$, $\partial \dot{y}_t/\partial x_{to}$, and $\partial \dot{z}_t/\partial x_{to}$. Similarly, the elements $\partial m_{1,E,t}/\partial x_{to}$, $\partial m_{2,E,t}/\partial x_{to}$, $\partial m_{3,E,t}/\partial x_{to}$, $\partial m_{1,M,t}/\partial x_{to}$, $\partial m_{2,M,t}/\partial x_{to}$, and $\partial m_{3,M,t}/\partial x_{to}$ of $\|M\|_{to,t}$ are computed. The remaining elements of the matrices $[\Phi]_{to,t}$ and $\|M\|_{to,t}$ are calculated from the parameters of trajectories 1, 3, 4, 5, and 6 and Δy_{to}, Δz_{to}, $\Delta \dot{x}_{to}$, $\Delta \dot{y}_{to}$, and $\Delta \dot{z}_{to}$. (See ref. 10 for a discussion of the transition matrices and their linearity.) For this study, $\Delta x_{to} = \Delta y_{to} = \Delta z_{to} = 1.6093440$ km and $\Delta \dot{x}_{to} = \Delta \dot{y}_{to} = \Delta \dot{z}_{to} = 0.003048$ km/sec were assumed.

In order to study a navigation scheme, isotropic deviations from the nominal of $\delta x = \delta y = \delta z = 9.6560640$ km ($\Delta r = 16.724795$ km) and of $\delta \dot{x} = \delta \dot{y} = \delta \dot{z} = 0.006096$ km/sec ($\Delta v = 0.010558583$ km/sec) were assumed to exist in the initial position and velocity components, respectively, for the purpose of computing the actual vehicular trajectory. The procedure is briefly as follows: A region was chosen on the reference trajectory and the transition matrices were computed; the actual path taken by the vehicle was then calculated; a particular combination of optical observations was assumed and the appropriate measurements were computed for the various points of the actual trajectory; measuring errors were generated by a Monte Carlo method for a prescribed standard deviation σ and added to the measurements to simulate actual onboard observations; and the data were weighted proportional to $1/\sigma$ and statistically reduced by equation (5). The procedure was then repeated for another combination of observations.

The star-to-horizon and angular-diameter (half-angle) measurement errors were assumed to vary with range. For the star-to-landmark or star-to-beacon and star-to-body-center measurements the error was assumed to be constant with range, the standard deviation of error being 5×10^{-5} radian (approximately 10 arc-seconds).

For the star-to-horizon and angular-diameter (half-angle) measurements, the variance for the earth measurements (in radians squared) was assumed to be

$$\sigma^2 = \left(5 \times 10^{-5}\right)^2 + \frac{4}{r^2 - R^2} \tag{7a}$$

and for the moon measurements to be

$$\sigma^2 = \left(5 \times 10^{-5}\right)^2 + \frac{0.25}{r^2 - R^2} \tag{7b}$$

RESULTS AND DISCUSSION

The results shown in tables III to VIII illustrate the accuracies obtainable from the optical navigation scheme for numerous combinations of various optical measurements. In figures 3 to 11 the results for some of the better combinations are shown.

Convergence of Mean of Measurement Error

Measurements were, in general, made at a fixed rate in particular regions of space for varied lengths of observing time (in hours). To these measurements, errors were added to simulate actual measurements and the resulting data were reduced to obtain the initial position and velocity error estimate at the beginning of each region.

Figure 3 shows both the error and the mean of the error in measuring the earth's subtended angle. The measurements cover the 4-hour interval beginning at earth insertion ($t = 0$) and are presented to show the behavior of the random measurement errors. The errors are seen to follow a trend, as would be expected from equation (7a). Near the earth the second term in equation (7a) is large (corresponding to a large value of σ); hence, the errors start with large values and then decrease rapidly to values which approach a constant value of σ $\left(5 \times 10^{-5}\text{ radian}\right)$. Results similar to those shown in figure 3 are obtained for measurements of angles between the earth horizon and stars in this region, starting at $t = 0$. For the other intervals and for the other types of measurements, the errors have a constant value of σ; thus, the initial values for the error and mean of the error would be lower than those shown in figure 3.

Convergence of Standard Deviation of Estimate

Figure 4 shows the convergence of root sum square of the standard deviations (root sum square of the standard deviations of the components) of the position and velocity error estimate as the number of measurements is increased. For this figure, a constant number of measurements was made per hour (25 combinations of observations per hour); however, the observing time is increased. It is evident that both the position and velocity estimate become more accurate as the period is lengthened. Also, the accuracy of the velocity estimate improves more rapidly than the position estimate with an increase in the interval of time over which the observations are made.

Since not only the total number of observations but also the interval of time over which the observations were made increases in figure 4, it is impossible to determine from these plots which variable is causing the increase in the accuracy of the estimates. Figure 5(a) shows the convergence of the standard deviation of the estimates as the number of measurements is increased and the time interval of observation is maintained constant at 2 hours. In figure 5(b) the convergence is shown as the observing time is increased and the number of observations is maintained constant at 40. It is evident from this figure that the standard deviation of the position error estimate for this combination of measuring instruments is a function of the number of measurements made and practically independent of the time rate of observation. However, the standard deviation of the velocity error estimate is a function of both the number of measurements and the rate of observation.

The standard deviations of the position error estimate and of the velocity error estimate improve slowly after about 40 position fixes (120 observations). After 4 hours, the standard deviation of the velocity error estimate will not improve greatly. Consequently, the results to be given in figures 6 to 11 pertain, for the most part, to a 4-hour observation period during which 40 individual combinations of 2 or 3 observations are made.

Estimated Error in Position and Velocity

In figure 6 the estimated error (root sum square of the components) in the position and velocity is plotted as a function of the total number of position fixes made (at a rate of 25 fixes per hour). The actual root sum squares of the errors given to the position and velocity vectors were 16.724795 km and 0.010558583 km/sec, respectively, and are shown as dashed horizontal lines in figure 6.

Figure 6 shows a random variation of the estimated errors in the position and velocity for the 4-hour measuring interval beginning 20 hours after insertion. If reference is made to figure 4, it will be seen that these random variations of the estimates are less than the standard deviations of the estimates.

In figure 6, the velocity error converges to the true value much more rapidly than the position error. The position error converges slowly for the first 30 to 40 groups of observations; whereas, the estimates of the velocity error converge quickly for this number of position fixes. Since one combination of observations is completed at the end of every 0.04 hour, 1.6 hours will have elapsed after 40 observations. From the results of figure 5(b), it is seen that the rapid initial convergence of the velocity estimate occurs within this period of 1.6 hours.

Even though the estimated errors in position and velocity have not converged sufficiently after 40 combinations of observations for satisfactory estimates of position and velocity, an increase in the specified number of 40 will not change the results of this report since the standard deviations have converged sufficiently (as evident from figs. 4, 5, and 9).

Accuracy of Various Measurement Combinations

In figure 7 the standard deviations of the position and velocity estimates for cases 400, 410, 430, 434, 438, and 439 are shown as a function of the radial distance from the earth's center. Smooth curves were drawn connecting the various values of σ_r and σ_v of the individual cases in order to show the variations more clearly. Cases 400, 410, and 430 are seen to start with small standard deviations and increase rapidly. In these cases, all measurements are made on the earth. Cases 434, 438, and 439 are the more accurate except for approximately the first 120,000 km. In these cases, all the position fixes are determined by measurements on both the earth and the moon.

The results shown in figures 8(a) and 8(b) are for cases which depend heavily on star-to-landmark and star-to-orbiting-beacon measurements. The curves are seen to have a wide variation. In general, the combinations which give the more accurate results over the greatest radial distance are those that involve the subtended angle of the earth (cases 440, 443, and 450). Since the remaining combinations contain the observation of the moon's subtended angle, greater accuracy near the moon is obtained with these observations.

At close earth range, using the star-to-landmark measurement results in much higher navigational accuracy than using the star-to-horizon measurement. (Compare cases 401 and 441 in table III.)

In figure 9 the root sum square of the standard deviation of the position and the velocity estimates for several of the more accurate combinations are plotted as a function of the number of hours of observation. The standard deviations are shown for the more accurate combination in each of the six regions studied. For the region beginning at insertion, $t = 0$ or $r = 6{,}465$ km, the most accurate combination (case 410) consisted of the subtended angle of the earth, the azimuth of the earth, and the elevation of the earth. (See table III.) This accuracy is equivalent to that obtained using angular diameter and two stars to body center since at least two stars must be sighted to aline the inertial platform used as a reference for azimuth and elevation. For example, case 410 (angular diameter, azimuth, and elevation) gives about the same accuracy as case 420 (angular diameter and two stars to body center). The contribution of angular diameter to the accuracy is small and these results are similar to those obtained for cases 411 and 421 where two-stars-to-body-center, elevation, and azimuth measurements are involved.

For the region beginning 1.5 hours after insertion, $r = 31{,}704$ km, the most accurate combination (case 430) consisted of the observation of the angles between the earth's horizon and three stars, as seen from the vehicle. (See table IV.) For the remaining intervals beginning 10, 20, 40, and 52 hours after insertion, the most accurate combination (case 439) consisted of the observation of the angle between the horizon of the earth and a star and the angles between the horizon of the moon and two stars. For cases 437, 438, and 439, which are identical except for stars selected, it is indicated in tables III to VIII that star selection is important.

No attempt was made to determine the optimum star locations for a given navigation system. However, the stars were selected to be approximately 20°, 40°, and 60° to the orbital plane; these angles thus gave fairly good measurement response to vehicle motions in the nominal trajectory plane and perpendicular to it.

In figure 10, the root sum square of the best estimate of errors for cases 410, 430, and 439 are plotted as a function of the number of hours of observation. The position fixes were made at a rate of 10 per hour and, as stated previously, the root-sum-square values of the vehicle actual position and velocity deviations from the nominal trajectory are 16.724795 km and 0.010558583 km/sec, respectively. The random curves of figure 10, in general, do not converge to the true errors. The curves for the 40-hour and 52-hour regions in figure 10(a) have a larger estimated deviation from the true error after 4 hours of observations than after 1 hour of observations. If reference is made to the standard deviations of the position and the velocity errors of figure 9, it can be seen that the random variation of the estimates of figure 10 lie well within the limits of the standard deviations.

In figure 11, the results of figure 9 are plotted as a function of the distance from the earth's center. The curves give a clearer picture of the variation of the convergence of the standard deviation (as observation period increases) over the earth-moon range. The standard deviations of the different combinations are drawn on a smooth curve; however, this does not mean that the standard deviations of the better combinations for other intervals will also lie on this curve. Two characteristics distinguish the curves of figure 11: the curves exhibit a maximum in standard deviation at $r = 120{,}700$ km (approximately 16 km for position and 0.0015 km/sec for velocity) and approach a limiting curve (along the entire distance) with an increase in the observation time.

SUMMARY OF RESULTS

On the basis of a standard deviation in instrument error of about 10 arc-seconds (except for horizon-type measurements near the earth or moon), the results of this study may be summarized as follows:

1. An observation period of 4 hours, during which approximately 40 position fixes were made, statistically determined vehicle position and velocity in space

within approximately 16 km and 0.0015 km/sec, respectively, in all regions of earth-moon space.

2. Certain combinations of observations were more suited for position and velocity determination in a particular region of space than others. The better of these combinations of observations studied are as follows: (a) Near the earth, the combination of optical measurements of the earth's angular diameter, azimuth, and elevation (or equivalently angular diameter and two stars to body center) was most accurate. The contribution of angular diameter to the accuracy in this region was, however, small and the use of only azimuth and elevation or two stars to body center gave approximately the same results. (b) For the region beginning 1.5 hours after insertion (a radial distance from earth's center to vehicle of 31,704 km), the most accurate combination consisted of the observation of the angles between the earth's horizon and three stars as seen from the spacecraft. (c) For the remainder of the trajectory up to the moon's sphere of influence, the most accurate combination consisted of the measurement of the angle between the horizon of the earth and one star and the angles between the horizon of the moon and two stars. In the terminal region within the moon's sphere of influence, measurements made solely on the moon would be expected to be of the highest accuracy. Results are not presented for this region; however, the results should be somewhat similar to those obtained by using measurements made on the earth at close range.

3. Because of the horizon indefinition at close range, the star-to-horizon measurement is much less effective than the star-to-landmark measurement.

Langley Research Center,
National Aeronautics and Space Administration,
Langley Station, Hampton, Va., March 16, 1964.

APPENDIX

Equations for Angles Corresponding to Various Optical Observations

The computer program used to obtain the spacecraft's position and velocity is outlined in figure 2. It is shown that a group of six types of onboard measurements used to determine the vehicle's position and velocity could be selected by the value of the computer logic control parameter K. Within this group of six measuring types, another combination was selected by assigning a weighting number of 1 to the measurements desired. A weighting number of zero would eliminate the measurement from the computations. The equations for the measurements as outlined in figure 2, for the various values of K, are given in the following table (the coordinates of the earth and moon center are measured in a vehicle-centered axis system):

	K = 0	K = 1	K = 2	K = 3	K = 4
$m_{1,E}$	$\sin^{-1} \frac{R_E}{\left(x_e^2 + y_e^2 + z_e^2\right)^{1/2}}$	$\sin^{-1} \frac{R_E}{\left(x_e^2 + y_e^2 + z_e^2\right)^{1/2}}$	$\sin^{-1} \frac{R_E}{\left(x_e^2 + y_e^2 + z_e^2\right)^{1/2}}$	$\cos^{-1} \frac{\left(a_1,b_1,c_1\right) \cdot \left(x_e,y_e,z_e\right)}{\left(x_e^2 + y_e^2 + z_e^2\right)^{1/2}} - \alpha_E$	$\sin^{-1} \frac{R_E}{\left(x_e^2 + y_e^2 + z_e^2\right)^{1/2}}$
$m_{2,E}$	$\cos^{-1} \frac{\left(a_1,b_1,c_1\right) \cdot \left(x_e,y_e,z_e\right)}{\left(x_e^2 + y_e^2 + z_e^2\right)^{1/2}} - \alpha_E$	$\sin^{-1} \frac{z}{\left(x_e^2 + y_e^2 + z_e^2\right)^{1/2}}$	$\cos^{-1} \frac{\left(a_1,b_1,c_1\right) \cdot \left(x_e,y_e,z_e\right)}{\left(x_e^2 + y_e^2 + z_e^2\right)^{1/2}}$	$\cos^{-1} \frac{\left(a_2,b_2,c_2\right) \cdot \left(x_e,y_e,z_e\right)}{\left(x_e^2 + y_e^2 + z_e^2\right)^{1/2}} - \alpha_E$	$\cos^{-1} \frac{\left(a_1,b_1,c_1\right) \cdot \left(x_e + \widehat{\Delta x}_E, y_e + \widehat{\Delta y}_E, z_e + \widehat{\Delta z}_E\right)}{\left[\left(x_e + \widehat{\Delta x}_E\right)^2 + \left(y_e + \widehat{\Delta y}_E\right)^2 + \left(z_e + \widehat{\Delta z}_E\right)^2\right]^{1/2}}$
$m_{3,E}$	$\cos^{-1} \frac{\left(a_2,b_2,c_2\right) \cdot \left(x_e,y_e,z_e\right)}{\left(x_e^2 + y_e^2 + z_e^2\right)^{1/2}} - \alpha_E$	$\tan^{-1} \frac{y_e}{x_e}$	$\cos^{-1} \frac{\left(a_2,b_2,c_2\right) \cdot \left(x_e,y_e,z_e\right)}{\left(x_e^2 + y_e^2 + z_e^2\right)^{1/2}}$	$\cos^{-1} \frac{\left(a_3,b_3,c_3\right) \cdot \left(x_e,y_e,z_e\right)}{\left(x_e^2 + y_e^2 + z_e^2\right)^{1/2}} - \alpha_E$	$\cos^{-1} \frac{\left(a_2,b_2,c_2\right) \cdot \left(x_e + \widehat{\Delta x}_E, y_e + \widehat{\Delta y}_E, z_e + \widehat{\Delta z}_E\right)}{\left[\left(x_e + \widehat{\Delta x}_E\right)^2 + \left(y_e + \widehat{\Delta y}_E\right)^2 + \left(z_e + \widehat{\Delta z}_E\right)^2\right]^{1/2}}$
$m_{1,M}$	$\sin^{-1} \frac{R_M}{\left(x_m^2 + y_m^2 + z_m^2\right)^{1/2}}$	$\sin^{-1} \frac{R_M}{\left(x_m^2 + y_m^2 + z_m^2\right)^{1/2}}$	$\sin^{-1} \frac{R_M}{\left(x_m^2 + y_m^2 + z_m^2\right)^{1/2}}$	$\cos^{-1} \frac{\left(a_1,b_1,c_1\right) \cdot \left(x_m,y_m,z_m\right)}{\left(x_m^2 + y_m^2 + z_m^2\right)^{1/2}} - \alpha_M$	$\sin^{-1} \frac{R_M}{\left(x_m^2 + y_m^2 + z_m^2\right)^{1/2}}$
$m_{2,M}$	$\cos^{-1} \frac{\left(a_1,b_1,c_1\right) \cdot \left(x_m,y_m,z_m\right)}{\left(x_m^2 + y_m^2 + z_m^2\right)^{1/2}} - \alpha_M$	$\sin^{-1} \frac{z_m}{\left(x_m^2 + y_m^2 + z_m^2\right)^{1/2}}$	$\cos^{-1} \frac{\left(a_1,b_1,c_1\right) \cdot \left(x_m,y_m,z_m\right)}{\left(x_m^2 + y_m^2 + z_m^2\right)^{1/2}}$	$\cos^{-1} \frac{\left(a_2,b_2,c_2\right) \cdot \left(x_m,y_m,z_m\right)}{\left(x_m^2 + y_m^2 + z_m^2\right)^{1/2}} - \alpha_M$	$\cos^{-1} \frac{\left(a_1,b_1,z_1\right) \cdot \left(x_m + \widehat{\Delta x}_M, y_m + \widehat{\Delta y}_M, z_m + \widehat{\Delta z}_M\right)}{\left[\left(x_m + \widehat{\Delta x}_M\right)^2 + \left(y_m + \widehat{\Delta y}_M\right)^2 + \left(z_m + \widehat{\Delta z}_M\right)^2\right]^{1/2}}$
$m_{3,M}$	$\cos^{-1} \frac{\left(a_2,b_2,c_2\right) \cdot \left(x_m,y_m,z_m\right)}{\left(x_m^2 + y_m^2 + z_m^2\right)^{1/2}} - \alpha_M$	$\tan^{-1} \frac{y_m}{x_m}$	$\cos^{-1} \frac{\left(a_2,b_2,c_2\right) \cdot \left(x_m,y_m,z_m\right)}{\left(x_m^2 + y_m^2 + z_m^2\right)^{1/2}}$	$\cos^{-1} \frac{\left(a_3,b_3,c_3\right) \cdot \left(x_m,y_m,z_m\right)}{\left(x_m^2 + y_m^2 + z_m^2\right)^{1/2}} - \alpha_M$	$\cos^{-1} \frac{\left(a_2,b_2,c_2\right) \cdot \left(x_m + \widehat{\Delta x}_M, y_m + \widehat{\Delta y}_M, z_m + \widehat{\Delta z}_M\right)}{\left[\left(x_m + \widehat{\Delta x}_M\right)^2 + \left(y_m + \widehat{\Delta y}_M\right)^2 + \left(z_m + \widehat{\Delta z}_M\right)^2\right]^{1/2}}$

The incremental changes $\hat{\Delta x}$, $\hat{\Delta y}$, and $\hat{\Delta z}$ in the equations of the foregoing table pertain to motions of the orbiting beacons and landmarks of the earth or moon. The orbiting beacon is in a circular orbit of radius R_B and inclination i. The ascending node of the beacon's orbit is on the X-axis. The landmarks are at latitude ϕ and at incremental longitude λ with respect to the X-axis at time zero. The spin axis and equatorial plane of the moon are assumed to be parallel to those of the earth and the selenocentric x, y, z coordinate system is assumed to be parallel to the geocentric system. Occultation of either the landmark or the beacon was assumed not to occur. The equations for the geocentric and selenocentric motions of the landmark and beacons are tabulated as follows:

Coordinates or landmarks	Coordinates or orbiting beacons
$\hat{\Delta x}_E = R_E \cos \phi_E \cos\left(\omega_E t + \lambda_E\right)$	$\hat{\Delta x}_E = R_{B,E} \cos\left(\omega_{s,E} t + \lambda_{s,E}\right)$
$\hat{\Delta y}_E = R_E \cos \phi_E \sin\left(\omega_E t + \lambda_E\right)$	$\hat{\Delta y}_E = R_{B,E} \sin\left(\omega_{s,E} t + \lambda_{s,E}\right) \cos i_E$
$\hat{\Delta z}_E = R_E \sin \phi_E$	$\hat{\Delta z}_E = R_{B,E} \sin\left(\omega_{s,E} t + \lambda_{s,E}\right) \sin i_E$
$\hat{\Delta x}_M = R_M \cos \phi_M \cos\left(\omega_M t + \lambda_M\right)$	$\hat{\Delta x}_M = R_{B,M} \cos\left(\omega_{s,M} t + \lambda_{s,M}\right)$
$\hat{\Delta y}_M = R_M \cos \phi_M \sin\left(\omega_M t + \lambda_M\right)$	$\hat{\Delta y}_M = R_{B,M} \sin\left(\omega_{s,M} t + \lambda_{s,M}\right) \cos i_M$
$\hat{\Delta z}_M = R_M \sin \phi_M$	$\hat{\Delta z}_M = R_{B,M} \sin\left(\omega_{s,M} t + \lambda_{s,M}\right) \sin i_M$

REFERENCES

1. Noton, A. R. M., Cutting, E., and Barnes, F. L.: Analysis of Radio-Command Mid-Course Guidance. Tech. Rep. No. 32-28 (Contract No. NASw-6), Jet Propulsion Lab., C.I.T., Sept. 8, 1960.

2. McLean, John D., Schmidt, Stanley F., and McGee, Leonard A.: Optimal Filtering and Linear Prediction Applied to a Midcourse Navigation System for the Circumlunar Mission. NASA TN D-1208, 1962.

3. Battin, Richard H.: A Statistical Optimizing Navigation Procedure for Space Flight. R-341 (Contracts NAS-9-103 and NAS-9-153), Instrumentation Lab., M.I.T., Sept. 1961.

4. Mayo, Alton P., Hamer, Harold A., and Hannah, Margery E.: Equations for Determining Vehicle Position in Earth-Moon Space From Simultaneous Onboard Optical Measurements. NASA TN D-1604, 1963.

5. Hamer, Harold A., and Mayo, Alton P.: Error Analysis of Several Methods of Determining Vehicle Position in Earth-Moon Space From Simultaneous Onboard Optical Measurements. NASA TN D-1805, 1963.

6. Hannah, Margery E., and Mayo, Alton P.: A Study of Factors Affecting the Accuracy of Position Fix for Lunar Trajectories. NASA TN D-2178, 1964.

7. Pines, Samuel, and Wolf, Henry: Interplanetary Trajectory by the Encke Method Programmed for the IBM 704. Rep. No. RAC-656-450 (Contract NASw-109 (NASA)), Republic Aviation Corp., Dec. 15, 1959.

8. Gainer, Patrick A.: A Method for Computing the Effect of an Additional Observation on a Previous Least-Squares Estimate. NASA TN D-1599, 1963.

9. Gapcynski, John P., and Woolston, Donald S.: Characteristics of Three Precision Circumlunar Trajectories for the Year 1968. NASA TN D-1028, 1962.

10. Jones, Ruben L., and Mayo, Alton P.: A Study of Some Transition Matrix Assumptions in Circumlunar Navigation Theory. NASA TN D-1812, 1963.

TABLE I.- POSITIONS OF THE THREE STARS SELECTED FOR OBSERVATION

Star	Direction cosines			Angle from orbit plane to star, deg
	a	b	c	
1	0.01399381	0.00779046	0.99987181	60.4
2	.20296362	.96862563	-.14341166	-37.2
3	.83337690	-.24094237	-.49741920	-21.0

TABLE II.- SELECTED COMBINATIONS OF ANGULAR OBSERVATIONS

Observation combination	Angles to be observed					
	$m_{1,E}$	$m_{2,E}$	$m_{3,E}$	$m_{1,M}$	$m_{2,M}$	$m_{3,M}$
0	X	X	X			
1		X	X			
2		X	X	X		
3	X	X				X
4	X		X		X	
5				X	X	X
6					X	X
7	X				X	X
8		X		X		X
9			X	X	X	

TABLE III.- ROOT SUM SQUARE OF STANDARD DEVIATIONS AND OF ESTIMATES OF POSITION AND VELOCITY ERRORS FOR EACH COMBINATION FOR THE REGION 0 HOUR AFTER INSERTION

Case	Description of observations			Δr, km	σ_r, km	Δv, km/sec	σ_v, km/sec
400	◯▷	$\ast_1$ ○̄	$\ast_2$ ○̄	21.566507	4.625866	1.257791×10^{-2}	3.982808×10^{-3}
401	$\ast_1$ ○̄	$\ast_2$ ○̄		34.451832	19.365951	2.664854×10^{-2}	16.995629×10^{-3}
402	$\ast_1$ ○̄	$\ast_2$ ○̄	☽▷	13.552697	19.343338	0.857077×10^{-2}	16.975681×10^{-3}
403	◯▷	$\ast_1$ ○̄	$\ast_2$ ☽	18.175933	5.020955	1.162413×10^{-2}	4.249581×10^{-3}
404	◯▷	$\ast_2$ ○̄	$\ast_1$ ☽	22.084643	4.949835	1.450771×10^{-2}	4.571649×10^{-3}
405	☽▷	$\ast_1$ ☽	$\ast_2$ ☽	79.637889	53.729116	3.519477×10^{-2}	37.778761×10^{-3}
406	$\ast_1$ ☽	$\ast_2$ ☽		45.715755	56.399388	3.201988×10^{-2}	38.050311×10^{-3}
407	◯▷	$\ast_1$ ☽	$\ast_2$ ☽	18.837927	5.631483	1.442097×10^{-2}	5.286241×10^{-3}
408	$\ast_1$ ○̄	☽▷	$\ast_2$ ☽	11.964933	30.705727	0.979655×10^{-2}	27.597659×10^{-3}
409	$\ast_2$ ○̄	☽▷	$\ast_1$ ☽	80.683814	62.840871	8.119767×10^{-2}	54.519309×10^{-3}
410	◯▷	Ⓔ	Ⓐ	16.626632	0.530105	1.077589×10^{-2}	0.663619×10^{-3}
411	Ⓔ	Ⓐ		16.775490	0.568877	1.050975×10^{-2}	0.723044×10^{-3}
412	Ⓔ	Ⓐ	☽▷	16.819845	0.568856	1.071234×10^{-2}	0.7230143×10^{-3}
413	◯▷	Ⓔ	A☽	15.765453	1.778232	1.0433956×10^{-2}	1.980917×10^{-3}
414	◯▷	Ⓐ	E☽	18.671838	2.039918	1.138237×10^{-2}	2.946561×10^{-3}
415	☽▷	E☽	A☽	20.345974	31.151486	1.554831×10^{-2}	20.985181×10^{-3}
416	E☽	A☽		43.613934	32.736062	2.378750×10^{-2}	21.491321×10^{-3}
417	◯▷	E☽	A☽	15.761566	5.571237	1.281333×10^{-2}	5.567244×10^{-3}
418	Ⓔ	☽▷	A☽	17.341454	10.249433	1.286297×10^{-2}	15.975636×10^{-3}
419	Ⓐ	☽▷	E☽	18.236058	2.3444434	1.145750×10^{-2}	3.368574×10^{-3}
420	◯▷	$\ast_1$ ⊕	$\ast_2$ ⊕	16.895178	0.764589	1.028771×10^{-2}	0.978503×10^{-3}
421	$\ast_1$ ⊕	$\ast_2$ ⊕		16.319468	0.961127	1.095465×10^{-2}	1.298651×10^{-3}
422	$\ast_1$ ⊕	$\ast_2$ ⊕	☽▷	16.701724	0.961075	1.035408×10^{-2}	1.298571×10^{-3}
423	◯▷	$\ast_1$ ⊕	$\ast_2$ ☽+	17.422390	1.840690	1.111813×10^{-2}	2.265754×10^{-3}
424	◯▷	$\ast_2$ ⊕	$\ast_1$ ☽+	17.089782	1.350038	1.136623×10^{-2}	2.294102×10^{-3}
425	☽▷	$\ast_1$ ☽+	$\ast_2$ ☽+	81.126894	54.929503	3.637823×10^{-2}	37.170721×10^{-3}
426	$\ast_1$ ☽+	$\ast_2$ ☽+		44.586362	58.401922	3.081336×10^{-2}	37.476987×10^{-3}

428	$\ast_1$ ⊕	⊳	$\ast_2$ ☽	15.654018	7.929552	1.206477×10^{-2}	12.890363×10^{-3}
429	$\ast_2$ ⊕	⊳	$\ast_1$ ☽	15.457845	2.645002	0.818720×10^{-2}	4.434839×10^{-3}
430	$\ast_1$ Ō	$\ast_2$ Ō	$\ast_3$ Ō	15.067736	2.926790	1.026437×10^{-2}	2.637337×10^{-3}
431	$\ast_2$ Ō	$\ast_3$ Ō		16.596394	4.203354	1.205681×10^{-2}	4.142905×10^{-3}
432	$\ast_2$ Ō	$\ast_3$ Ō	$\ast_1$ ☽	20.169879	4.106468	1.294351×10^{-2}	4.015841×10^{-3}
433	$\ast_1$ Ō	$\ast_2$ Ō	$\ast_3$ ☽	24.200419	13.195367	1.599003×10^{-2}	11.068702×10^{-3}
434	$\ast_1$ Ō	$\ast_3$ Ō	$\ast_2$ ☽	18.434113	3.311627	1.063626×10^{-2}	3.095191×10^{-3}
435	$\ast_1$ ☽	$\ast_2$ ☽	$\ast_3$ ☽	44.591443	28.084770	1.983575×10^{-2}	20.417274×10^{-3}
436	$\ast_2$ ☽	$\ast_3$ ☽		22.959824	35.507708	2.553652×10^{-2}	22.628109×10^{-3}
437	$\ast_1$ Ō	$\ast_2$ ☽	$\ast_3$ ☽	23.565734	17.933358	1.433514×10^{-2}	14.428650×10^{-3}
438	$\ast_2$ Ō	$\ast_1$ ☽	$\ast_3$ ☽	12.459890	22.246677	0.815412×10^{-2}	19.249531×10^{-3}
439	$\ast_3$ Ō	$\ast_1$ ☽	$\ast_2$ ☽	17.762484	5.258338	1.027983×10^{-2}	5.858241×10^{-3}
440	○▷	$\ast_1$ Ⓛ	$\ast_2$ Ⓛ	16.902750	1.552342	1.023847×10^{-2}	1.849464×10^{-3}
441	$\ast_1$ Ⓛ	$\ast_2$ Ⓛ		16.168658	2.555888	1.052293×10^{-2}	3.214870×10^{-3}
442	$\ast_1$ Ⓛ	$\ast_2$ Ⓛ	⊳	16.916087	2.555565	1.099527×10^{-2}	3.214430×10^{-3}
443	○▷	$\ast_1$ Ⓛ	$\ast_2$ L☽	17.905101	2.508537	1.134891×10^{-2}	2.828998×10^{-3}
444	○▷	$\ast_2$ Ⓛ	$\ast_1$ L☽	16.759131	2.088958	1.087704×10^{-2}	2.915048×10^{-3}
445	⊳	$\ast_1$ L☽	$\ast_2$ L☽	92.318692	54.685419	3.932995×10^{-2}	36.479919×10^{-3}
446	$\ast_1$ L☽	$\ast_2$ L☽		38.462844	58.465865	2.853853×10^{-2}	36.831482×10^{-3}
447	○▷	$\ast_1$ L☽	$\ast_2$ L☽	18.567652	5.626562	1.423811×10^{-2}	5.277380×10^{-3}
448	$\ast_1$ Ⓛ	⊳	$\ast_2$ L☽	14.587563	7.302003	0.848795×10^{-2}	11.171733×10^{-3}
449	$\ast_2$ Ⓛ	⊳	$\ast_1$ L☽	15.287832	5.610614	0.853073×10^{-2}	7.801853×10^{-3}
450	○▷	$\ast_1$ ∅	$\ast_2$ ∅	17.143863	1.443402	1.029481×10^{-2}	1.619968×10^{-3}
451	$\ast_1$ ∅	$\ast_2$ ∅		15.997641	1.671104	1.055024×10^{-2}	1.945468×10^{-3}
452	$\ast_1$ ∅	$\ast_2$ ∅	⊳	17.054474	1.671040	1.083555×10^{-2}	1.945377×10^{-3}
453	○▷	$\ast_1$ ∅	$\ast_2$ ♄	17.984782	2.289578	1.181242×10^{-2}	2.424969×10^{-3}
454	○▷	$\ast_2$ ∅	$\ast_1$ ♄	16.894401	2.085485	1.065328×10^{-2}	2.354483×10^{-3}
455	⊳	$\ast_1$ ♄	$\ast_2$ ♄	72.621613	49.780547	3.206012×10^{-2}	36.741663×10^{-3}
456	$\ast_1$ ♄	$\ast_2$ ♄		38.837394	50.958579	2.979893×10^{-2}	36.895845×10^{-3}
457	$\ast_1$ ♄	♄	○▷	18.645092	5.620894	1.419135×10^{-2}	5.244855×10^{-3}
458	$\ast_1$ ∅	⊳	$\ast_2$ ♄	17.199069	3.016118	1.121802×10^{-2}	3.278488×10^{-3}
459	$\ast_2$ ∅	⊳	$\ast_1$ ♄	18.599554	2.894006	1.318647×10^{-2}	3.4295434×10^{-3}

TABLE IV.- ROOT SUM SQUARE OF STANDARD DEVIATIONS AND OF ESTIMATES OF POSITION AND VELOCITY ERRORS FOR EACH COMBINATION FOR THE REGION 1.5 HOURS AFTER INSERTION

Case	Description of observations			Δr, km	σ_r, km	Δv, km/sec	σ_v, km/sec
400		$\ast_1$	$\ast_2$	27.68200	8.966267	0.856096×10^{-2}	1.706967×10^{-3}
401	$\ast_1$	$\ast_2$		145.71660	109.43925	0.380660×10^{-2}	10.804765×10^{-3}
402	$\ast_1$	$\ast_2$		75.068823	108.453726	0.578901×10^{-2}	10.710892×10^{-3}
403		$\ast_1$	$\ast_2$	24.858376	10.917870	1.043529×10^{-2}	1.779130×10^{-3}
404		$\ast_2$	$\ast_1$	23.986374	10.544840	0.913740×10^{-2}	1.857682×10^{-3}
405		$\ast_1$	$\ast_2$	20.856294	327.801164	2.049812×10^{-2}	51.616664×10^{-3}
406	$\ast_1$	$\ast_2$		40.229055	348.551418	0.302509×10^{-2}	56.642405×10^{-3}
407		$\ast_1$	$\ast_2$	32.278212	12.887047	0.772357×10^{-2}	1.931276×10^{-3}
408	$\ast_1$		$\ast_2$	207.415908	178.841361	1.231454×10^{-2}	23.067498×10^{-3}
409	$\ast_2$		$\ast_1$	49.468887	257.125358	0.660853×10^{-2}	29.363386×10^{-3}
410		E	A	15.465157	5.535017	1.095083×10^{-2}	0.9179006×10^{-3}
411	E	A		156.059990	65.862706	1.483596×10^{-2}	3.763290×10^{-3}
412	E	A		46.120252	63.977076	0.998444×10^{-2}	3.662706×10^{-3}
413		E	A	21.629588	8.942545	1.058705×10^{-2}	1.653891×10^{-3}
414		A	E	23.837520	7.329307	0.903136×10^{-2}	1.052005×10^{-3}
415		E	A	124.298612	442.729183	0.301759×10^{-2}	63.444799×10^{-3}
416	E	A		154.545477	496.179986	2.340387×10^{-2}	70.709228×10^{-3}
417		E	A	29.645913	10.329784	0.825610×10^{-2}	1.753863×10^{-3}
418	E		A	50.017752	45.339168	1.690503×10^{-2}	16.806577×10^{-3}
419	A		E	45.883598	64.258658	0.971464×10^{-2}	3.586922×10^{-3}
420		$\ast_1$	$\ast_2$	26.805802	7.693239	0.834747×10^{-2}	1.548820×10^{-3}
421	$\ast_1$	$\ast_2$		178.438832	209.16858	1.446981×10^{-2}	15.073118×10^{-3}
422	$\ast_1$	$\ast_2$		70.875389	158.60523	1.178956×10^{-2}	11.65039×10^{-3}
423		$\ast_1$	$\ast_2$	24.309709	10.202899	1.035977×10^{-2}	1.727298×10^{-3}
424		$\ast_2$	$\ast_1$	25.025256	9.705820	0.883132×10^{-2}	1.787747×10^{-3}
425		$\ast_1$	$\ast_2$	317.00808	381.71298	6.426524×10^{-2}	57.692773×10^{-3}
426	$\ast_1$	$\ast_2$		36.181933	416.47367	0.295685×10^{-2}	63.66779×10^{-3}
427		$\ast_1$	$\ast_2$	32.306280	12.861674	0.773988×10^{-2}	1.924788×10^{-3}

428	$\ast_1$ ⊕	⊳	$\ast_2$ ☽	42.485426	58.590800	1.032309×10^{-2}	22.441510×10^{-3}
429	$\ast_2$ ⊕	⊳	$\ast_1$ ☽	67.664722	50.546814	0.398894×10^{-2}	9.495816×10^{-3}
430	$\ast_1$ ◯	$\ast_2$ ◯	$\ast_3$ ◯	13.683165	3.186399	1.164889×10^{-2}	0.648413×10^{-3}
431	$\ast_2$ ◯	$\ast_3$ ◯		55.104510	18.592758	1.371291×10^{-2}	2.012605×10^{-3}
432	$\ast_2$ ◯	$\ast_3$ ◯	$\ast_1$ ☽	28.502443	13.297748	1.123370×10^{-2}	1.597537×10^{-3}
433	$\ast_1$ ◯	$\ast_2$ ◯	$\ast_3$ ☽	10.736080	10.019628	1.147839×10^{-2}	1.483873×10^{-3}
434	$\ast_1$ ◯	$\ast_3$ ◯	$\ast_2$ ☽	15.513604	10.076992	0.915562×10^{-2}	1.358458×10^{-3}
435	$\ast_1$ ☽	$\ast_2$ ☽	$\ast_3$ ☽	457.592520	275.557432	5.316490×10^{-2}	39.649360×10^{-3}
436	$\ast_2$ ☽	$\ast_3$ ☽		390.369208	340.981015	7.198395×10^{-2}	46.957518×10^{-3}
437	$\ast_1$ ◯	$\ast_2$ ☽	$\ast_3$ ☽	42.616784	23.956218	1.820013×10^{-2}	3.748911×10^{-3}
438	$\ast_2$ ◯	$\ast_1$ ☽	$\ast_3$ ☽	160.365552	48.064190	0.448815×10^{-2}	5.749779×10^{-3}
439	$\ast_3$ ◯	$\ast_1$ ☽	$\ast_2$ ☽	33.758897	11.508684	1.124409×10^{-2}	1.248368×10^{-3}
440	⊳	$\ast_1$ Ⓛ	$\ast_2$ Ⓛ	26.534864	7.232029	0.837184×10^{-2}	1.4184195×10^{-3}
441	$\ast_1$ Ⓛ	$\ast_2$ Ⓛ		207.792971	102.749683	1.383071×10^{-2}	7.918697×10^{-3}
442	$\ast_1$ Ⓛ	$\ast_2$ Ⓛ	⊳	66.413042	94.404280	1.235134×10^{-2}	7.328244×10^{-3}
443	⊳	$\ast_1$ Ⓛ	$\ast_2$ L☽	24.093811	9.980170	1.033238×10^{-2}	1.714305×10^{-3}
444	⊳	$\ast_2$ Ⓛ	$\ast_1$ L☽	27.286910	9.372546	0.845330×10^{-2}	1.702670×10^{-3}
445	⊳	$\ast_1$ L☽	$\ast_2$ L☽	218.873954	455.878746	5.407770×10^{-2}	72.310404×10^{-3}
446	$\ast_1$ L☽	$\ast_2$ L		195.940400	516.351295	2.386233×10^{-2}	85.097894×10^{-3}
447	⊳	$\ast_1$ L	$\ast_2$ L☽	32.454514	12.877134	0.772770×10^{-2}	1.924663×10^{-3}
448	$\ast_1$ Ⓛ	⊳	$\ast_2$ L☽	33.957963	34.805045	0.566404×10^{-2}	18.340237×10^{-3}
449	$\ast_2$ Ⓛ	⊳	$\ast_1$ L☽	32.874620	30.976750	0.612292×10^{-2}	8.026716×10^{-3}
450	⊳	$\ast_1$ ♄	$\ast_2$ ♄	27.344686	6.325510	0.795284×10^{-2}	1.282473×10^{-3}
451	$\ast_1$ ♄	$\ast_2$ ♄		14.510489	9.556467	1.163286×10^{-2}	1.968314×10^{-3}
452	$\ast_1$ ♄	$\ast_2$ ♄	⊳	22.733593	9.557525	0.849702×10^{-2}	1.967835×10^{-3}
453	⊳	$\ast_1$ ♄	$\ast_2$ ♄	22.141194	8.800987	1.079967×10^{-2}	1.559100×10^{-3}
454	⊳	$\ast_2$ ♄	$\ast_1$ ♄	22.459683	8.334664	1.008794×10^{-2}	1.544259×10^{-3}
455	⊳	$\ast_1$ ♄	$\ast_2$ ♄	18.893578	369.204950	1.849530×10^{-2}	18.558897×10^{-3}
456	$\ast_1$ ♄	$\ast_2$ ♄		275.406974	411.241353	2.214684×10^{-2}	51.701465×10^{-3}
457	$\ast_1$ ♄	♄	⊳	32.260266	12.888592	0.774128×10^{-2}	1.916035×10^{-3}
458	$\ast_1$ ♄	⊳	$\ast_2$ ♄	30.960721	14.844155	0.908026×10^{-2}	3.190347×10^{-3}
459	$\ast_2$ ♄	⊳	$\ast_1$ ♄	39.294054	19.672299	0.738714×10^{-2}	3.394831×10^{-3}

TABLE V.- ROOT SUM SQUARE OF STANDARD DEVIATIONS AND OF ESTIMATES OF POSITION AND VELOCITY ERRORS FOR EACH COMBINATION FOR THE REGION 10 HOURS AFTER INSERTION

Case	Description of observations			Δr, km	σ_r, km	Δv, km/sec	σ_v, km/sec
400	○>	$*_1$ Ō	$*_2$ Ō	38.301951	56.854837	0.906633×10^{-2}	6.960940×10^{-3}
401	$*_1$ Ō	$*_2$ Ō		422.398292	547.808563	1.836516×10^{-2}	51.779673×10^{-3}
402	$*_1$ Ō	$*_2$ Ō	☽>	102.695871	206.840793	1.582891×10^{-2}	21.281700×10^{-3}
403	○>	$*_1$ Ō	$*_2$ ☽	60.058793	46.773955	0.866553×10^{-2}	6.478360×10^{-3}
404	○>	$*_2$ Ō	$*_1$ ☽	88.001663	83.764696	1.533121×10^{-2}	12.954407×10^{-3}
405	☽>	$*_1$ ☽	$*_2$ ☽	527.881794	342.171029	4.660214×10^{-2}	43.399807×10^{-3}
406	$*_1$ ☽	$*_2$ ☽		73.206303	460.876483	0.429294×10^{-2}	77.388762×10^{-3}
407	○>	$*_1$ ☽	$*_2$ ☽	51.540371	51.615549	0.315615×10^{-2}	7.169690×10^{-3}
408	$*_1$ Ō	☽>	$*_2$ ☽	471.682971	279.037638	0.778039×10^{-2}	30.357268×10^{-3}
409	$*_2$ Ō	☽>	$*_1$ ☽	210.647278	297.187949	1.568832×10^{-2}	18.049264×10^{-3}
410	○>	Ⓔ	Ⓐ	40.145599	40.939030	0.748442×10^{-2}	5.501927×10^{-3}
411	Ⓔ	Ⓐ		505.813649	697.040811	3.317858×10^{-2}	19.198164×10^{-3}
412	Ⓔ	Ⓐ	☽>	178.528730	289.336281	0.677716×10^{-2}	15.100490×10^{-3}
413	○>	Ⓔ	A☽	73.318618	49.568072	0.680954×10^{-2}	6.863660×10^{-3}
414	○>	Ⓐ	E☽	45.378369	41.461710	0.645902×10^{-2}	5.544586×10^{-3}
415	☽>	E☽	A☽	396.483122	337.477618	1.247111×10^{-2}	38.019658×10^{-3}
416	E☽	A☽		70.724677	469.427459	1.046209×10^{-2}	48.208789×10^{-3}
417	○>	E☽	A☽	58.896087	50.681736	0.430988×10^{-2}	7.025316×10^{-3}
418	Ⓔ	☽>	A☽	147.076574	306.343603	2.422772×10^{-2}	32.226927×10^{-3}
419	Ⓐ	☽>	E☽	280.525895	286.838515	0.834150×10^{-2}	13.796920×10^{-3}
420	○>	$*_1$ ⊕	$*_2$ ⊕	67.317646	48.578139	0.981043×10^{-2}	6.391901×10^{-3}
421	$*_1$ ⊕	$*_2$ ⊕		766.798439	530.115902	15.046966×10^{-2}	$134.599154 \times 10^{-3}$
422	$*_1$ ⊕	$*_2$ ⊕	☽>	31.106342	388.582385	2.436187×10^{-2}	52.626510×10^{-3}
423	○>	$*_1$ ⊕	$*_2$ ☽̶	63.341746	48.159931	0.826178×10^{-2}	6.675396×10^{-3}
424	○>	$*_2$ ⊕	$*_1$ ☽̶	82.806628	90.193946	1.457532×10^{-2}	12.523592×10^{-3}
425	☽>	$*_1$ ☽̶	$*_2$ ☽̶	495.434635	381.873803	4.280417×10^{-2}	45.818107×10^{-3}
426	$*_1$ ☽̶	$*_2$ ☽̶		245.851517	600.696725	0.748953×10^{-2}	79.255044×10^{-3}
427	○>	$*_1$ ☽̶	$*_2$ ☽̶	54.123809	51.238470	0.296101×10^{-2}	71.048059×10^{-3}

428	$\ast_1$	⊕	☽▷		$\ast_2$	☽̶	554.194585	321.699803	1.601397×10^{-2}	36.058368×10^{-3}
429	$\ast_2$	⊕	☽▷		$\ast_1$	☽̶	239.783549	307.296818	1.483431×10^{-2}	16.217242×10^{-3}
430	$\ast_1$	Ō	$\ast_2$	Ō	$\ast_3$	Ō	13.967714	32.245959	1.457202×10^{-2}	4.488138×10^{-3}
431	$\ast_2$	Ō	$\ast_3$	Ō			352.072614	541.585970	1.688747×10^{-2}	20.872793×10^{-3}
432	$\ast_2$	Ō	$\ast_3$	Ō	$\ast_1$	☽	16.359698	28.250812	13.145144×10^{-2}	3.277248×10^{-3}
433	$\ast_1$	Ō	$\ast_2$	Ō	$\ast_3$	☽	93.299530	107.538775	2.396110×10^{-2}	10.808557×10^{-3}
434	$\ast_1$	Ō	$\ast_3$	Ō	$\ast_2$	☽	89.709490	29.555482	1.346083×10^{-2}	3.314691×10^{-3}
435	$\ast_1$	☽	$\ast_2$	☽	$\ast_3$	☽	36.006042	264.236856	0.446363×10^{-2}	29.667631×10^{-3}
436	$\ast_2$	☽	$\ast_3$	☽			612.017204	470.627531	6.015060×10^{-2}	47.505308×10^{-3}
437	$\ast_1$	Ō	$\ast_2$	☽	$\ast_3$	☽	96.449384	46.357918	2.185673×10^{-2}	6.143514×10^{-3}
438	$\ast_2$	Ō	$\ast_1$	☽	$\ast_3$	☽	78.916877	49.219380	1.816710×10^{-2}	5.308049×10^{-3}
439	$\ast_3$	Ō	$\ast_1$	☽	$\ast_2$	☽	11.464176	14.789891	1.228339×10^{-2}	1.720057×10^{-3}
440	○▷		$\ast_1$	Ⓛ	$\ast_2$	Ⓛ	130.169532	73.664023	1.753702×10^{-2}	8.022887×10^{-3}
441	$\ast_1$	Ⓛ	$\ast_2$	Ⓛ			557.865643	553.745192	10.613982×10^{-2}	99.658939×10^{-3}
442	$\ast_1$	Ⓛ	$\ast_2$	Ⓛ	☽▷		225.223718	324.079926	1.043828×10^{-2}	42.473702×10^{-3}
443	○▷		$\ast_1$	Ⓛ	$\ast_2$	L☽	66.361575	47.084447	0.806991×10^{-2}	6.519030×10^{-3}
444	○▷		$\ast_2$	Ⓛ	$\ast_1$	L☽	74.186629	63.198487	0.951121×10^{-2}	8.074956×10^{-3}
445	☽▷		$\ast_1$	L☽	$\ast_2$	L☽	441.742735	328.591545	3.738393×10^{-2}	42.604956×10^{-3}
446	$\ast_1$	L☽	$\ast_2$	L☽			860.855776	433.147696	0.801917×10^{-2}	80.343388×10^{-3}
447	○▷		$\ast_1$	L☽	$\ast_2$	L☽	50.600001	50.953217	0.332854×10^{-2}	7.071670×10^{-3}
448	$\ast_1$	Ⓛ	☽▷		$\ast_2$	L☽	753.975910	257.626926	1.501141×10^{-2}	23.489705×10^{-3}
449	$\ast_2$	Ⓛ	☽▷		$\ast_1$	L☽	406.686620	316.480845	2.312676×10^{-2}	14.645536×10^{-3}
450	○▷		$\ast_1$	🪐	$\ast_2$	🪐	79.143489	43.772409	0.995216×10^{-2}	5.774830×10^{-3}
451	$\ast_1$	🪐	$\ast_2$	🪐			114.056773	95.272799	0.508697×10^{-2}	12.453270×10^{-3}
452	$\ast_1$	🪐	$\ast_2$	🪐	☽▷		19.733478	94.476202	0.761530×10^{-2}	12.321690×10^{-3}
453	○▷		$\ast_1$	🪐	$\ast_2$	⚵	47.534626	44.033152	0.818670×10^{-2}	6.113374×10^{-3}
454	○▷		$\ast_2$	🪐	$\ast_1$	⚵	23.576014	35.449339	1.221409×10^{-2}	4.743305×10^{-3}
455	☽▷		$\ast_1$	⚵	$\ast_2$	⚵	572.291256	329.929553	2.145932×10^{-2}	33.849492×10^{-3}
456	$\ast_1$	⚵	$\ast_2$				527.484431	477.671871	2.789040×10^{-2}	39.396323×10^{-3}
457	$\ast_1$	⚵	⚵		○▷		63.664202	50.487970	0.230703×10^{-2}	7.026370×10^{-3}
458	$\ast_1$	🪐	☽▷		$\ast_2$	⚵	102.652686	108.050965	0.206193×10^{-2}	14.360011×10^{-3}
459	$\ast_2$	🪐	☽▷		$\ast_1$	⚵	1.043639	37.945486	0.905754×10^{-2}	4.947032×10^{-3}

TABLE VI.- ROOT SUM SQUARE OF STANDARD DEVIATIONS AND OF ESTIMATES OF POSITION AND VELOCITY ERRORS FOR EACH COMBINATION FOR THE REGION 20 HOURS AFTER INSERTION

Case	Description of observations			Δr, km	σ_r, km	Δv, km/sec	σ_v, km/sec
400		$\ast_1$	$\ast_2$	102.963082	94.84730	0.847593×10^{-2}	12.276194×10^{-3}
401	$\ast_1$	$\ast_2$		1001.1385	631.481834	8.305396×10^{-2}	91.446547×10^{-3}
402	$\ast_1$	$\ast_2$		35.996928	335.339444	1.481908×10^{-2}	12.858267×10^{-3}
403		$\ast_1$	$\ast_2$	126.005943	111.059960	0.413238×10^{-2}	14.755790×10^{-3}
404		$\ast_2$	$\ast_1$	101.031246	273.253463	1.149448×10^{-2}	30.804099×10^{-3}
405		$\ast_1$	$\ast_2$	25.840603	264.800609	1.390600×10^{-2}	33.129328×10^{-3}
406	$\ast_1$	$\ast_2$		212.560401	406.062146	1.494588×10^{-2}	91.375639×10^{-3}
407		$\ast_1$	$\ast_2$	119.80995	120.346459	0.952959×10^{-2}	15.966221×10^{-3}
408	$\ast_1$		$\ast_2$	86.360331	253.570429	1.787605×10^{-2}	31.700472×10^{-3}
409	$\ast_2$		$\ast_1$	162.604304	498.056965	4.420742×10^{-2}	47.489006×10^{-3}
410		E	A	94.006869	90.305595	0.795678×10^{-2}	11.663495×10^{-3}
411	E	A		365.68354	739.20976	7.276515×10^{-2}	50.554886×10^{-3}
412	E	A		260.07910	320.78796	2.986400×10^{-2}	34.822760×10^{-3}
413		E	A	16.728621	117.37217	0.261082×10^{-2}	15.385184×10^{-3}
414		A	E	62.387595	92.439723	0.703800×10^{-2}	12.015668×10^{-3}
415		E	A	423.40970	272.21771	2.060781×10^{-2}	32.323626×10^{-3}
416	E	A		906.82651	462.03151	0.4667001×10^{-2}	59.135989×10^{-3}
417		E	A	73.477803	118.65208	0.468310×10^{-2}	15.577613×10^{-3}
418	E		A	537.43191	277.94196	1.969530×10^{-2}	32.557930×10^{-3}
419	A		E	15.773254	303.69356	2.917675×10^{-2}	31.606132×10^{-3}
420		$\ast_1$	$\ast_2$	121.827141	93.182522	2.735315×10^{-2}	12.063884×10^{-3}
421	$\ast_1$	$\ast_2$		911.212177	691.821323	25.087758×10^{-2}	$211.250701 \times 10^{-3}$
422	$\ast_1$	$\ast_2$		65.348124	398.229952	0.908924×10^{-2}	$157.139245 \times 10^{-3}$
423		$\ast_1$	$\ast_2$	158.696094	115.624876	0.241938×10^{-2}	15.271194×10^{-3}
424		$\ast_2$	$\ast_1$	224.249110	296.515420	1.621537×10^{-2}	32.389834×10^{-3}
425		$\ast_1$	$\ast_2$	421.871429	297.04118	2.932370×10^{-2}	35.788061×10^{-3}
426	$\ast_1$	$\ast_2$		85.397570	558.81623	1.826949×10^{-2}	95.616679×10^{-3}
427		$\ast_1$	$\ast_2$	125.92611	120.956821	0.987846×10^{-2}	15.932947×10^{-3}

428	$*_1$ ⊖	)>	$*_2$ ☽	405.02613	288.96855	1.242038 × 10^{-2}	34.870139 × 10^{-3}
429	$*_2$ ⊖	)>	$*_1$ ☽	19.104462	454.43645	4.513503 × 10^{-2}	43.017862 × 10^{-3}
430	$*_1$ Ō	$*_2$ Ō	$*_3$ Ō	15.053012	79.422552	2.119559 × 10^{-2}	10.432959 × 10^{-3}
431	$*_2$ Ō	$*_3$ Ō		628.38989	572.81418	4.758985 × 10^{-2}	168.17848 × 10^{-3}
432	$*_2$ Ō	$*_3$ Ō	$*_1$ ☽	13.199389	20.398770	0.213851 × 10^{-2}	2.478840 × 10^{-3}
433	$*_1$ Ō	$*_2$ Ō	$*_3$ ☽	42.145935	27.259712	0.967356 × 10^{-2}	3.194997 × 10^{-3}
434	$*_1$ Ō	$*_3$ Ō	$*_2$ ☽	12.656887	16.270308	2.044289 × 10^{-2}	1.949904 × 10^{-3}
435	$*_1$ ☽	$*_2$ ☽	$*_3$ ☽	63.174458	174.45765	0.480565 × 10^{-2}	20.225511 × 10^{-3}
436	$*_2$ ☽	$*_3$ ☽		287.52589	389.08808	4.081634 × 10^{-2}	56.962956 × 10^{-3}
437	$*_1$ Ō	$*_2$ ☽	$*_3$ ☽	190.55286	98.557244	3.243754 × 10^{-2}	13.485804 × 10^{-3}
438	$*_2$ Ō	$*_1$ ☽	$*_3$ ☽	21.447159	21.320473	1.353849 × 10^{-2}	2.515823 × 10^{-3}
439	$*_3$ Ō	$*_1$ ☽	$*_2$ ☽	16.232312	9.565294	1.075428 × 10^{-2}	1.144712 × 10^{-3}
440	○>	$*_1$ Ⓛ	$*_2$ Ⓛ	110.07425	93.267761	153.79968 × 10^{-2}	12.097358 × 10^{-3}
441	$*_1$ Ⓛ	$*_2$ Ⓛ		163.90412	692.43305	436.50136 × 10^{-2}	124.241220 × 10^{-3}
442	$*_1$ Ⓛ	$*_2$ Ⓛ	)>	448.41055	367.46127	582.19572 × 10^{-2}	45.111611 × 10^{-3}
443	○>	$*_1$ Ⓛ	$*_2$ L☽	112.90564	109.99745	58.478170 × 10^{-2}	14.460109 × 10^{-3}
444	○>	$*_2$ Ⓛ	$*_1$ L☽	365.57569	350.86153	203.66211 × 10^{-2}	23.51733 × 10^{-3}
445	)>	$*_1$ L☽	$*_2$ L☽	388.87310	270.662371	254.58285 × 10^{-2}	33.34231 × 10^{-3}
446	$*_1$ L☽	$*_2$ L☽		83.926002	462.77821	288.93572 × 10^{-2}	98.049428 × 10^{-3}
447	○>	$*_1$ L☽	$*_2$ L☽	66.044581	118.28863	39.254894 × 10^{-2}	15.617340 × 10^{-3}
448	$*_1$ Ⓛ	)>	$*_2$ L☽	635.10635	243.43694	310.76735 × 10^{-2}	28.371198 × 10^{-3}
449	$*_2$ Ⓛ	)>	$*_1$ L☽	196.901532	380.468153	139.08408 × 10^{-2}	23.766929 × 10^{-3}
450	○>	$*_1$ ♄	$*_2$ ♄	124.63000	84.542783	137.09586 × 10^{-2}	10.919125 × 10^{-3}
451	$*_1$ ♄	$*_2$ ♄		305.289016	188.44252	355.29530 × 10^{-2}	24.01205 × 10^{-3}
452	$*_1$ ♄	$*_2$ ♄	)>	18.525159	176.09514	121.018259 × 10^{-2}	22.214250 × 10^{-3}
453	○>	$*_1$ ♄	$*_2$ ⚳	24.476673	96.055789	79.173883 × 10^{-2}	12.593938 × 10^{-3}
454	○>	$*_2$ ♄	$*_1$ ⚳	30.668464	81.125261	115.45294 × 10^{-2}	10.784295 × 10^{-3}
455	)>	$*_1$ ⚳	$*_2$ ⚳	329.84648	229.0723	253.83365 × 10^{-2}	22.767325 × 10^{-3}
456	$*_1$ ⚳	$*_2$ ⚳		575.20755	456.42653	171.14593 × 10^{-2}	27.410790 × 10^{-3}
457	$*_1$ ⚳	⚳	○>	97.229483	109.83362	66.335599 × 10^{-2}	14.020090 × 10^{-3}
458	$*_1$ ♄	)>	$*_2$ ⚳	168.57782	156.412385	34.03188 × 10^{-2}	19.064933 × 10^{-3}
459	$*_2$ ♄	)>	$*_1$ ⚳	20.615037	82.554841	134.08243 × 10^{-2}	11.105125 × 10^{-3}

TABLE VII.- ROOT SUM SQUARE OF STANDARD DEVIATIONS AND OF ESTIMATES OF POSITION AND VELOCITY ERRORS FOR EACH COMBINATION FOR THE REGION 40 HOURS AFTER INSERTION

Case	Description of observations			Δr, km	σ_r, km	Δv, km/sec	σ_v, km/sec
400		$*_1$	$*_2$	160.686527	190.100718	1.973968×10^{-2}	24.329054×10^{-3}
401	$*_1$	$*_2$		319.229183	575.014169	20.095379×10^{-2}	$289.850660 \times 10^{-3}$
402	$*_1$	$*_2$		199.993839	182.302755	1.883216×10^{-2}	21.444839×10^{-3}
403		$*_1$	$*_2$	109.980564	231.215032	1.678979×10^{-2}	30.938179×10^{-3}
404		$*_2$	$*_1$	30.375024	326.761656	1.312279×10^{-2}	41.252303×10^{-3}
405		$*_1$	$*_2$	248.379024	121.221709	1.195198×10^{-2}	14.038403×10^{-3}
406	$*_1$	$*_2$		124.821162	383.444732	0.6995627×10^{-2}	62.488552×10^{-3}
407		$*_1$	$*_2$	212.207376	227.548834	2.594079×10^{-2}	30.020281×10^{-3}
408	$*_1$		$*_2$	336.983807	122.234012	1.627109×10^{-2}	14.178926×10^{-3}
409	$*_2$		$*_1$	93.923204	457.717760	3.493791×10^{-2}	53.810961×10^{-3}
410		E	A	157.550646	191.654395	1.873054×10^{-2}	24.279362×10^{-3}
411	E	A		85.969224	745.013441	20.927188×10^{-2}	$156.987429 \times 10^{-3}$
412	E	A		119.516252	202.753365	1.369044×10^{-2}	23.672485×10^{-3}
413		E	A	444.021743	247.342944	2.353271×10^{-2}	31.212833×10^{-3}
414		A	E	125.778119	194.448731	1.532005×10^{-2}	24.545296×10^{-3}
415		E	A	145.716710	123.553828	0.376925×10^{-2}	14.233468×10^{-3}
416	E	A		230.489797	423.466606	1.672547×10^{-2}	52.048892×10^{-3}
417		E	A	68.905161	239.561846	0.625252×10^{-2}	30.278230×10^{-3}
418	E		A	316.69532	124.738084	1.407857×10^{-2}	14.364108×10^{-3}
419	A		E	204.342528	204.963847	3.369394×10^{-2}	23.891072×10^{-3}
420		$*_1$	$*_2$	200.125580	190.905712	2.487311×10^{-2}	24.394298×10^{-3}
421	$*_1$	$*_2$		320.792004	647.563252	38.422407×10^{-2}	$448.270991 \times 10^{-3}$
422	$*_1$	$*_2$		223.294243	202.374638	2.249746×10^{-2}	23.822649×10^{-3}
423		$*_1$	$*_2$	211.759833	259.440930	0.314866×10^{-2}	34.079932×10^{-3}
424		$*_2$	$*_1$	71.428247	343.748878	1.121000×10^{-2}	43.342899×10^{-3}
425		$*_1$	$*_2$	232.223897	124.865991	1.019029×10^{-2}	14.433350×10^{-3}
426	$*_1$	$*_2$		212.999736	452.169096	1.757466×10^{-2}	73.829990×10^{-3}
427		$*_1$	$*_2$	208.791108	248.851591	2.647911×10^{-2}	32.411366×10^{-3}

428	$*_1$ ⊕	☽>	$*_2$ ☽+	368.627163	126.013269	1.960055×10^{-2}	14.576602×10^{-3}
429	$*_2$ ⊕	☽>	$*_1$ ☽+	72.548817	406.531318	3.057407×10^{-2}	47.423816×10^{-3}
430	$*_1$ Ō	$*_2$ Ō	$*_3$ Ō	40.595038	183.572173	2.837235×10^{-2}	24.750834×10^{-3}
431	$*_2$ Ō	$*_3$ Ō		256.838250	468.484110	13.798589×10^{-2}	$163.317195 \times 10^{-3}$
432	$*_2$ Ō	$*_3$ Ō	$*_1$ ☽	10.919567	20.350258	1.146184×10^{-2}	2.562820×10^{-3}
433	$*_1$ Ō	$*_2$ Ō	$*_3$ ☽	35.536058	18.171985	0.974067×10^{-2}	2.251124×10^{-3}
434	$*_1$ Ō	$*_3$ Ō	$*_2$ ☽	16.806563	12.957175	1.007040×10^{-2}	1.585701×10^{-3}
435	$*_1$ ☽	$*_2$ ☽	$*_3$ ☽	59.408940	72.722031	0.626407×10^{-2}	8.396802×10^{-3}
436	$*_2$ ☽	$*_3$ ☽		209.919773	372.202450	3.586625×10^{-2}	47.592889×10^{-3}
437	$*_1$ Ō	$*_2$ ☽	$*_3$ ☽	318.582407	190.958322	2.697170×10^{-2}	21.496098×10^{-3}
438	$*_2$ Ō	$*_1$ ☽	$*_3$ ☽	10.196480	14.079558	1.151124×10^{-2}	1.711733×10^{-3}
439	$*_3$ Ō	$*_1$ ☽	$*_2$ ☽	22.152442	7.823455	0.947511×10^{-2}	0.874180×10^{-3}
440	○>	$*_1$ Ⓛ	$*_2$ Ⓛ	170.377194	190.338370	2.160062×10^{-2}	24.286903×10^{-3}
441	$*_1$ Ⓛ	$*_2$ Ⓛ		1149.772067	600.389581	15.602063×10^{-2}	$212.939257 \times 10^{-3}$
442	$*_1$ Ⓛ	$*_2$ Ⓛ	☽>	287.643412	196.764062	2.896601×10^{-2}	$23.2563372 \times 10^{-3}$
443	○>	$*_1$ Ⓛ	$*_2$ L☽	301.428071	262.024169	0.866055×10^{-2}	33.900503×10^{-3}
444	○>	$*_2$ Ⓛ	$*_1$ L☽	18.345955	341.483163	1.180518×10^{-2}	40.309336×10^{-3}
445	☽>	$*_1$ L☽	$*_2$ L☽	214.613876	126.355546	0.853109×10^{-2}	14.596637×10^{-3}
446	$*_1$ L☽	$*_2$ L☽		15.748008	490.814337	1.824448×10^{-2}	79.723913×10^{-3}
447	○>	$*_1$ L☽	$*_2$ L☽	266.136831	259.238684	3.265782×10^{-2}	33.634554×10^{-3}
448	$*_1$ Ⓛ	☽>	$*_2$ L☽	350.359982	126.891383	1.771845×10^{-2}	14.640247×10^{-3}
449	$*_2$ Ⓛ	☽>	$*_1$ L☽	103.490797	350.946041	4.066245×10^{-2}	40.630588×10^{-3}
450	○>	$*_1$ Ø	$*_2$ Ø	167.425094	172.928793	2.231824×10^{-2}	21.695803×10^{-3}
451	$*_1$ Ø	$*_2$ Ø		862.041428	340.461793	10.955416×10^{-2}	42.264676×10^{-3}
452	$*_1$ Ø	$*_2$ Ø	☽>	76.250229	180.908210	1.347199×10^{-2}	21.263707×10^{-3}
453	○>	$*_1$ Ø	$*_2$ ϑ	70.636133	182.795842	0.369058×10^{-2}	16.631931×10^{-3}
454	○>	$*_2$ Ø	$*_1$ ϑ	16.757310	204.730894	1.061457×10^{-2}	25.943242×10^{-3}
455	☽>	$*_1$ ϑ	$*_2$ ϑ	196.180981	90.019456	0.749902×10^{-2}	8.565794×10^{-3}
456	$*_1$ ϑ	$*_2$ ϑ		127.560595	287.926013	1.191234×10^{-2}	10.602111×10^{-3}
457	$*_1$ ϑ	ϑ	○>	55.547324	160.694392	0.447041×10^{-2}	10.085351×10^{-3}
458	$*_1$ Ø	☽>	$*_2$ ϑ	262.811653	110.134927	0.860293×10^{-2}	11.711577×10^{-3}
459	$*_2$ Ø	☽>	$*_1$ ϑ	39.879697	217.916942	4.289862×10^{-2}	27.093168×10^{-3}

TABLE VIII.- ROOT SUM SQUARE OF STANDARD DEVIATIONS AND OF ESTIMATES OF POSITION AND VELOCITY ERRORS FOR EACH COMBINATION FOR THE REGION 52 HOURS AFTER INSERTION

Case	Description of observations			Δr, km	σ_r, km	Δv, km/sec	σ_v, km/sec
400		*1	*2	150.95663	244.20186	2.207746×10^{-2}	31.201318×10^{-3}
401	*1	*2		392.26473	644.79172	15.622997×10^{-2}	436.02601×10^{-3}
402	*1	*2		95.354437	84.275703	0.790008×10^{-2}	9.541350×10^{-3}
403		*1	*2	217.58975	227.51779	0.497437×10^{-2}	20.070106×10^{-3}
404		*2	*1	17.022751	370.957477	1.773051×10^{-2}	47.338532×10^{-3}
405		*1	*2	77.975131	48.414217	0.561709×10^{-2}	5.333307×10^{-3}
406	*1	*2		184.118336	320.525223	0.408579×10^{-2}	19.476494×10^{-3}
407		*1	*2	154.654563	219.171249	0.387404×10^{-2}	18.011696×10^{-3}
408	*1		*2	145.51399	49.599660	0.436747×10^{-2}	5.497503×10^{-3}
409	*2		*1	145.313367	196.646323	2.279409×10^{-2}	21.677059×10^{-3}
410		E	A	316.81224	243.80596	3.839122×10^{-2}	31.064202×10^{-3}
411	E	A		54.715443	664.54642	32.713618×10^{-2}	238.58364×10^{-3}
412	E	A		89.392783	90.563581	0.837269×10^{-2}	10.160159×10^{-3}
413		E	A)	95.632209	228.73928	0.618344×10^{-2}	19.873950×10^{-3}
414		A	E)	37.926123	234.10483	0.878430×10^{-2}	28.155473×10^{-3}
415		E)	A)	59.352768	48.795954	0.767948×10^{-2}	5.374887×10^{-3}
416	E)	A)		190.63484	311.126429	0.640023×10^{-2}	20.212073×10^{-3}
417		E)	A)	25.568936	222.55135	1.292949×10^{-2}	19.097442×10^{-3}
418	E		A)	148.96265	49.226936	0.420840×10^{-2}	5.434014×10^{-3}
419	A		E)	72.026191	95.991415	1.000484×10^{-2}	10.734003×10^{-3}
420		*1	*2	184.41473	246.40183	2.648320×10^{-2}	31.409084×10^{-3}
421	*1	*2		447.38154	700.20948	15.405349×10^{-2}	587.40090×10^{-3}
422	*1	*2		110.09313	93.471182	0.931656×10^{-2}	10.588421×10^{-3}
423		*1	*2	162.36833	240.12539	0.567176×10^{-2}	25.660346×10^{-3}
424		*2	*1	17.922692	372.562895	1.686409×10^{-2}	46.505391×10^{-3}
425		*1	*2	74.299278	49.140418	0.590513×10^{-2}	5.430941×10^{-3}
426	*1	*2		141.648200	335.276744	0.609945×10^{-2}	26.201086×10^{-3}
427		*1	*2	133.129601	228.380687	0.628948×10^{-2}	23.008635×10^{-3}

428	$\star_1$	⊕			$\star_2$		144.58781	50.070876	0.426486×10^{-2}	5.558948×10^{-3}
429	$\star_2$				$\star_1$		128.243802	170.014672	1.960397×10^{-2}	18.721660×10^{-3}
430	$\star_1$		$\star_2$		$\star_3$		73.950934	233.119369	4.786477×10^{-2}	31.912122×10^{-3}
431	$\star_2$		$\star_3$				229.380010	449.001987	25.347010×10^{-2}	$257.882860 \times 10^{-3}$
432	$\star_2$		$\star_3$		$\star_1$		9.748538	21.941196	1.107885×10^{-2}	2.698107×10^{-3}
433	$\star_1$		$\star_2$		$\star_3$		35.604045	17.688834	0.963290×10^{-2}	2.159167×10^{-3}
434	$\star_1$		$\star_3$		$\star_2$		18.178249	12.566972	0.970022×10^{-2}	1.532545×10^{-3}
435	$\star_1$		$\star_2$		$\star_3$		32.989202	28.664975	0.882187×10^{-2}	3.166958×10^{-3}
436	$\star_2$		$\star_3$				289.371976	293.204339	1.647819×10^{-2}	17.064172×10^{-3}
437	$\star_1$		$\star_2$		$\star_3$		102.069705	80.713156	0.411986×10^{-2}	8.941466×10^{-3}
438	$\star_2$		$\star_1$		$\star_3$		14.473712	13.062939	1.090369×10^{-2}	1.588739×10^{-3}
439	$\star_3$		$\star_1$		$\star_2$		23.873604	6.710529	0.910839×10^{-2}	0.820615×10^{-3}
440			$\star_1$	L	$\star_2$	L	243.04152	249.24554	3.204047×10^{-2}	31.603976×10^{-3}
441	$\star_1$	L	$\star_2$	L			316.09126	778.25140	5.630226×10^{-2}	269.78351×10^{-3}
442	$\star_1$	L	$\star_2$	L			99.356392	91.709755	0.876709×10^{-2}	10.396250×10^{-3}
443			$\star_1$	L	$\star_2$	L	242.46377	268.20040	0.347488×10^{-2}	28.405404×10^{-3}
444			$\star_2$	L	$\star_1$	L	119.98078	381.98585	0.973333×10^{-2}	45.434678×10^{-3}
445			$\star_1$	L	$\star_2$	L	73.576794	49.587107	0.597194×10^{-2}	5.481892×10^{-3}
446	$\star_1$	L	$\star_2$	L			362.85235	397.66247	1.291972×10^{-2}	29.889381×10^{-3}
447			$\star_1$	L	$\star_2$	L	101.238700	258.18384	0.649853×10^{-2}	26.338363×10^{-3}
448	$\star_1$	L			$\star_2$	L	149.21097	50.385020	0.409394×10^{-2}	5.593388×10^{-3}
449	$\star_2$	L			$\star_1$	L	105.765283	160.61832	1.690519×10^{-2}	18.040585×10^{-3}
450			$\star_1$		$\star_2$		405.667342	225.84729	4.941797×10^{-2}	28.453363×10^{-3}
451	$\star_1$		$\star_2$				283.730566	438.74741	6.394873×10^{-2}	56.470111×10^{-3}
452	$\star_1$		$\star_2$				107.35387	91.900945	0.967233×10^{-2}	10.399581×10^{-3}
453			$\star_1$		$\star_2$		88.852687	185.41252	1.215847×10^{-2}	8.656565×10^{-3}
454			$\star_2$		$\star_1$		151.60053	253.112941	1.599859×10^{-2}	30.877840×10^{-3}
455			$\star_1$		$\star_2$		84.655518	33.567697	0.513028×10^{-2}	2.916566×10^{-3}
456	$\star_1$		$\star_2$				17.825577	149.95481	0.988934×10^{-2}	4.180047×10^{-3}
457	$\star_1$						61.941237	131.41163	0.874263×10^{-2}	3.977317×10^{-3}
458	$\star_1$				$\star_2$		120.26064	43.376327	0.446706×10^{-2}	4.322440×10^{-3}
459	$\star_2$				$\star_1$		98.952608	158.84306	2.472950×10^{-2}	17.454784×10^{-3}

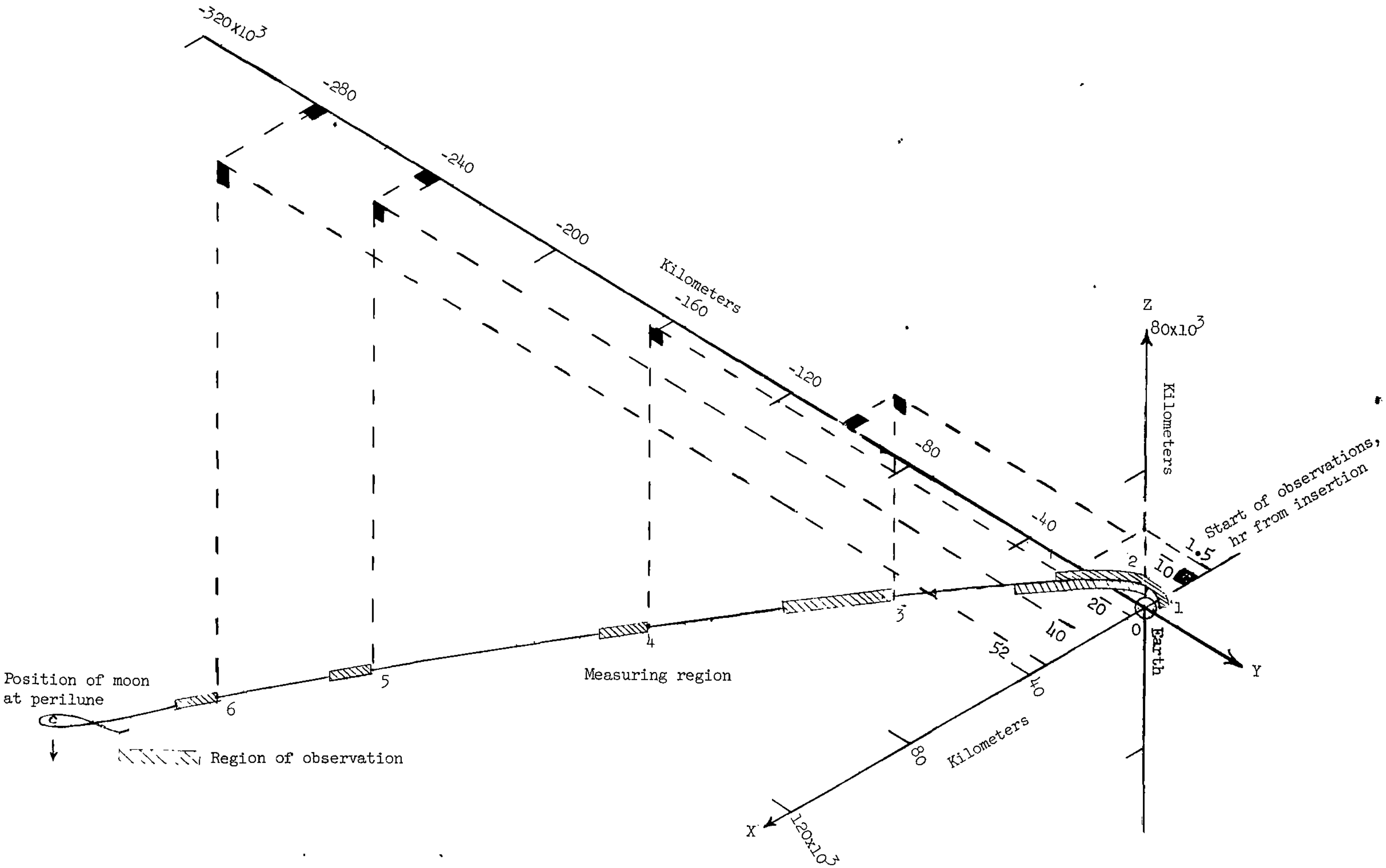

Figure 1.- Plot of trajectory illustrating the regions where navigation measurements were made.

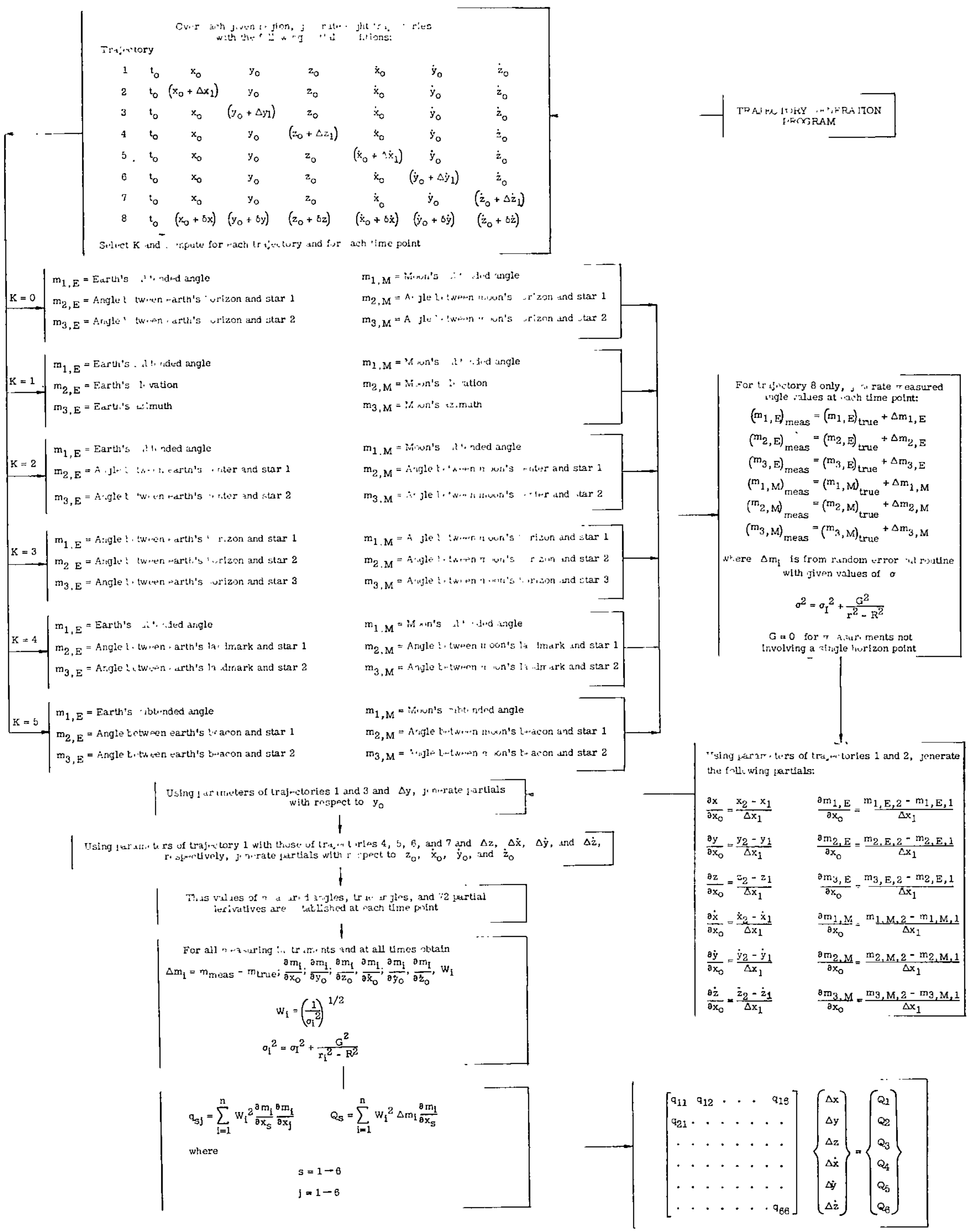

Figure 2.- Block diagram of computational procedure.

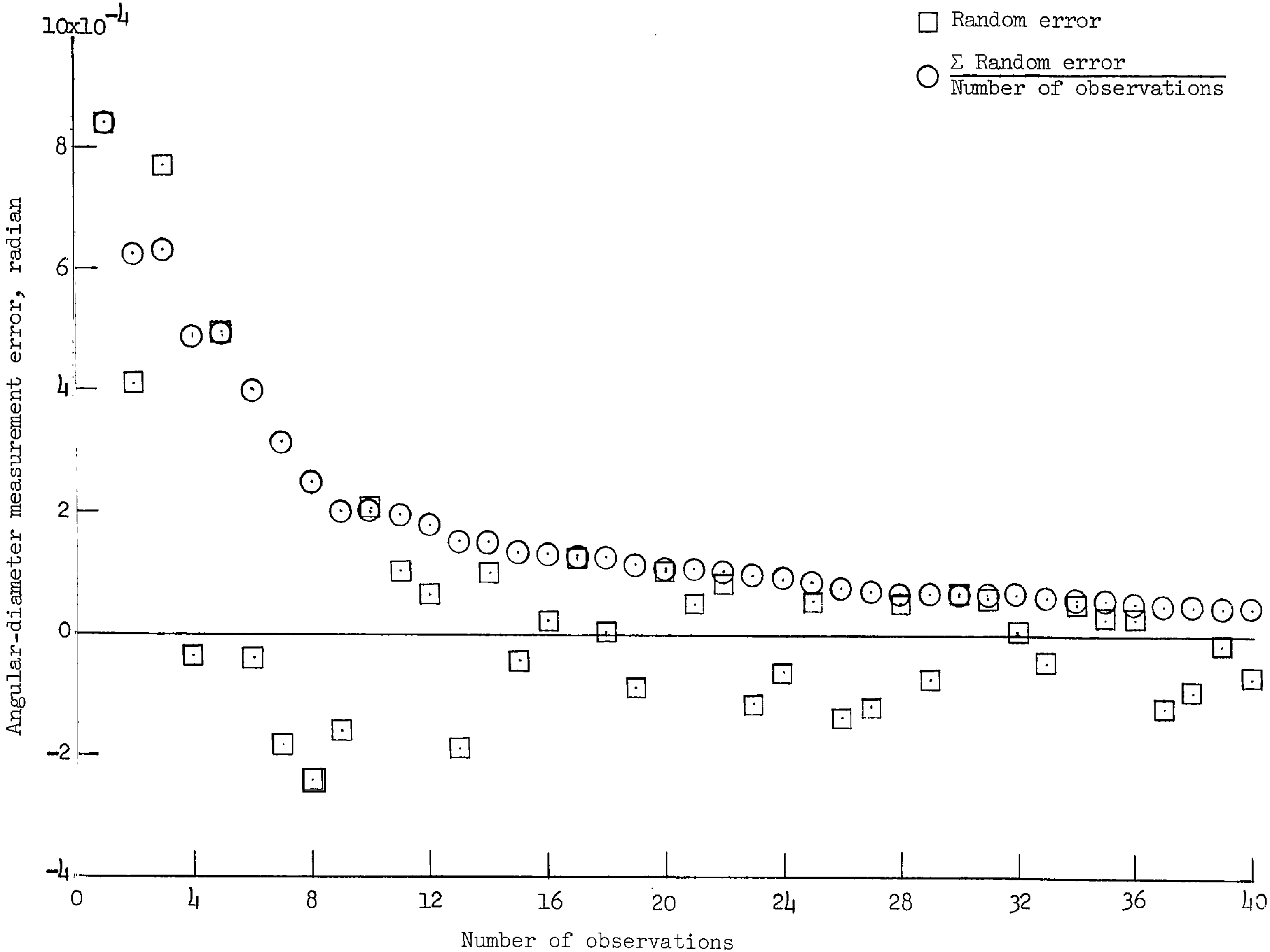

Figure 3.- Measurement error for the earth's subtended angle as a function of the number of observations.

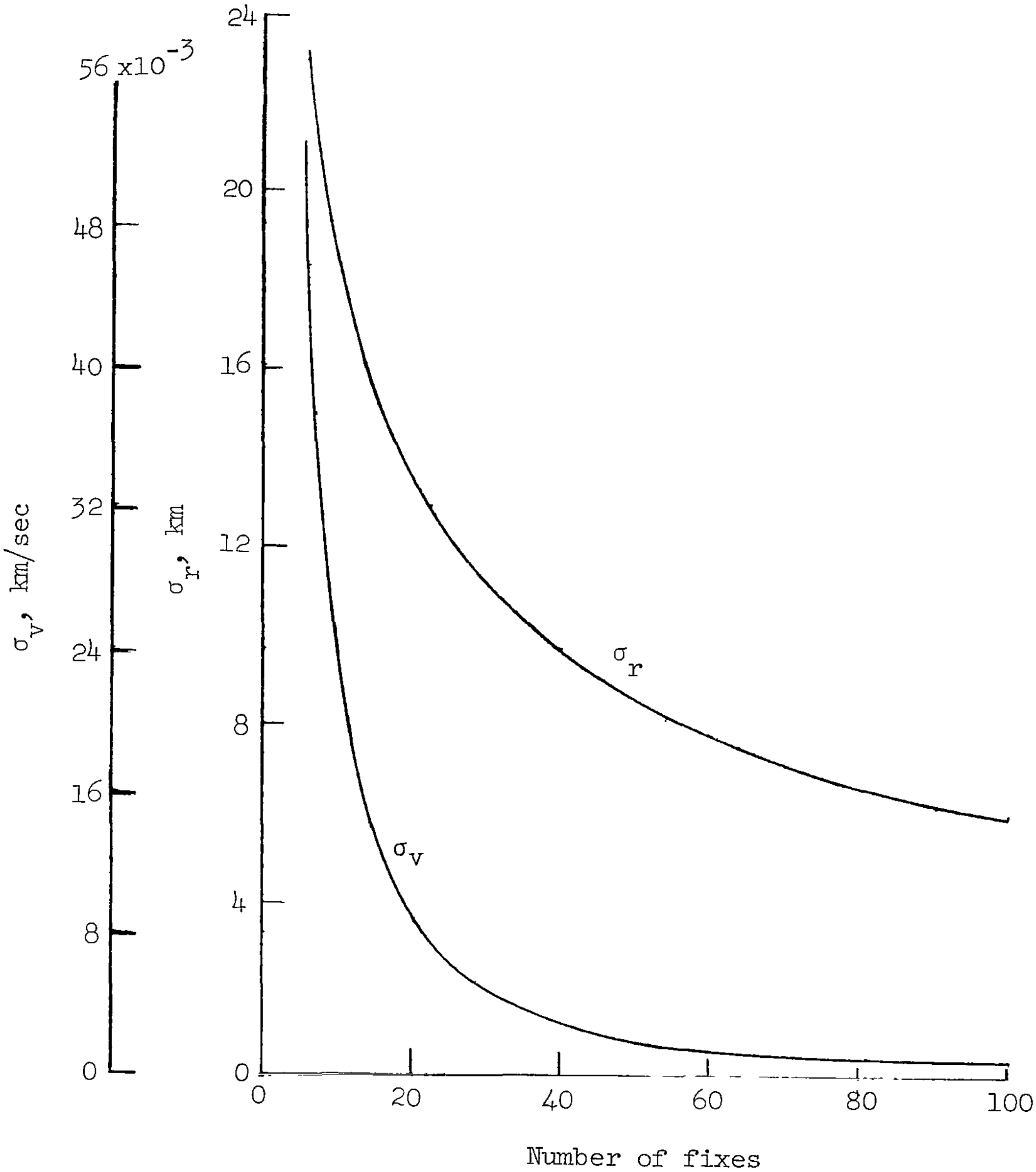

Figure 4.- Root sum square of standard deviations of errors in position and velocity for case 439 (20 hours after insertion) as a function of the number of fixes (fixes taken 25 per hour).

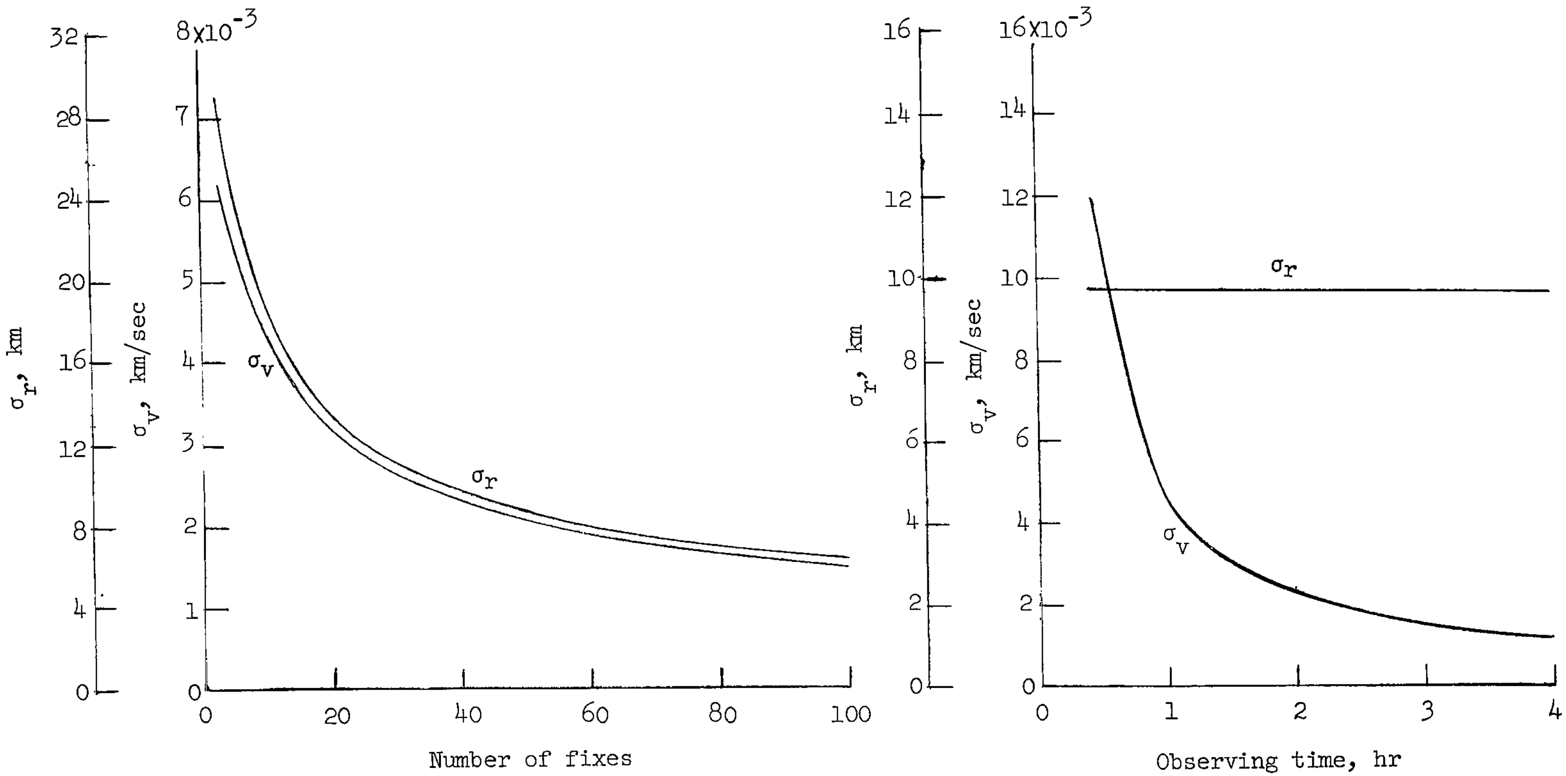

(a) Constant observing time (2 hr).

(b) Constant number of fixes (40).

Figure 5.- Effect of number of fixes and observing time on the root sum square of standard deviations of errors in position and velocity for case 439 (20 hours after insertion).

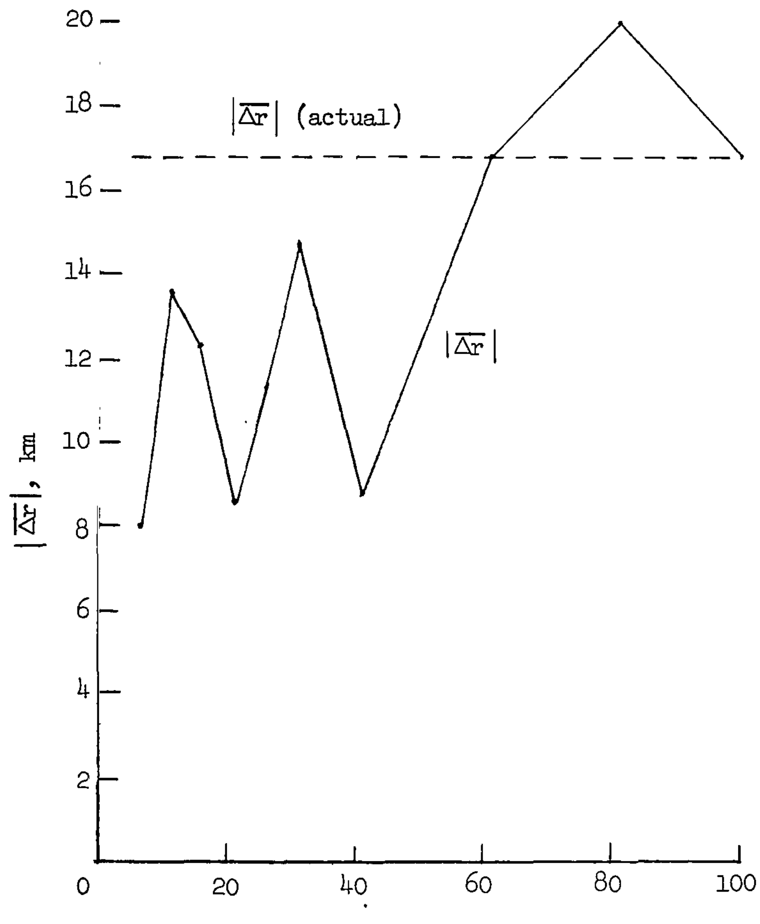

(a) Position.

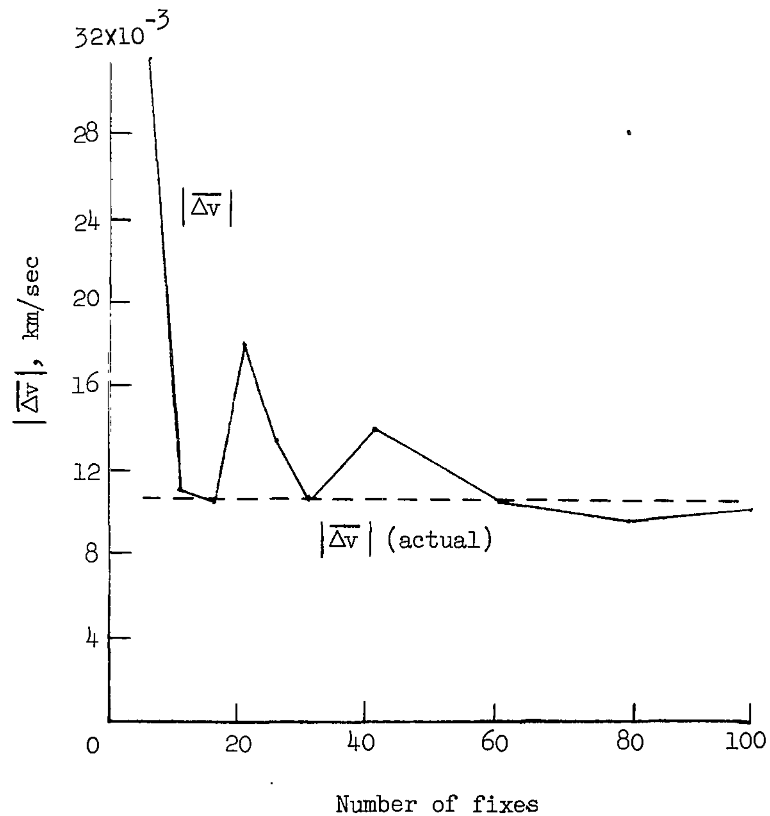

(b) Velocity.

Figure 6.- Root sum square of best estimates of errors in velocity and position for case 439 (20 hours after insertion) as a function of the number of fixes (fixes taken at 25 per hour).

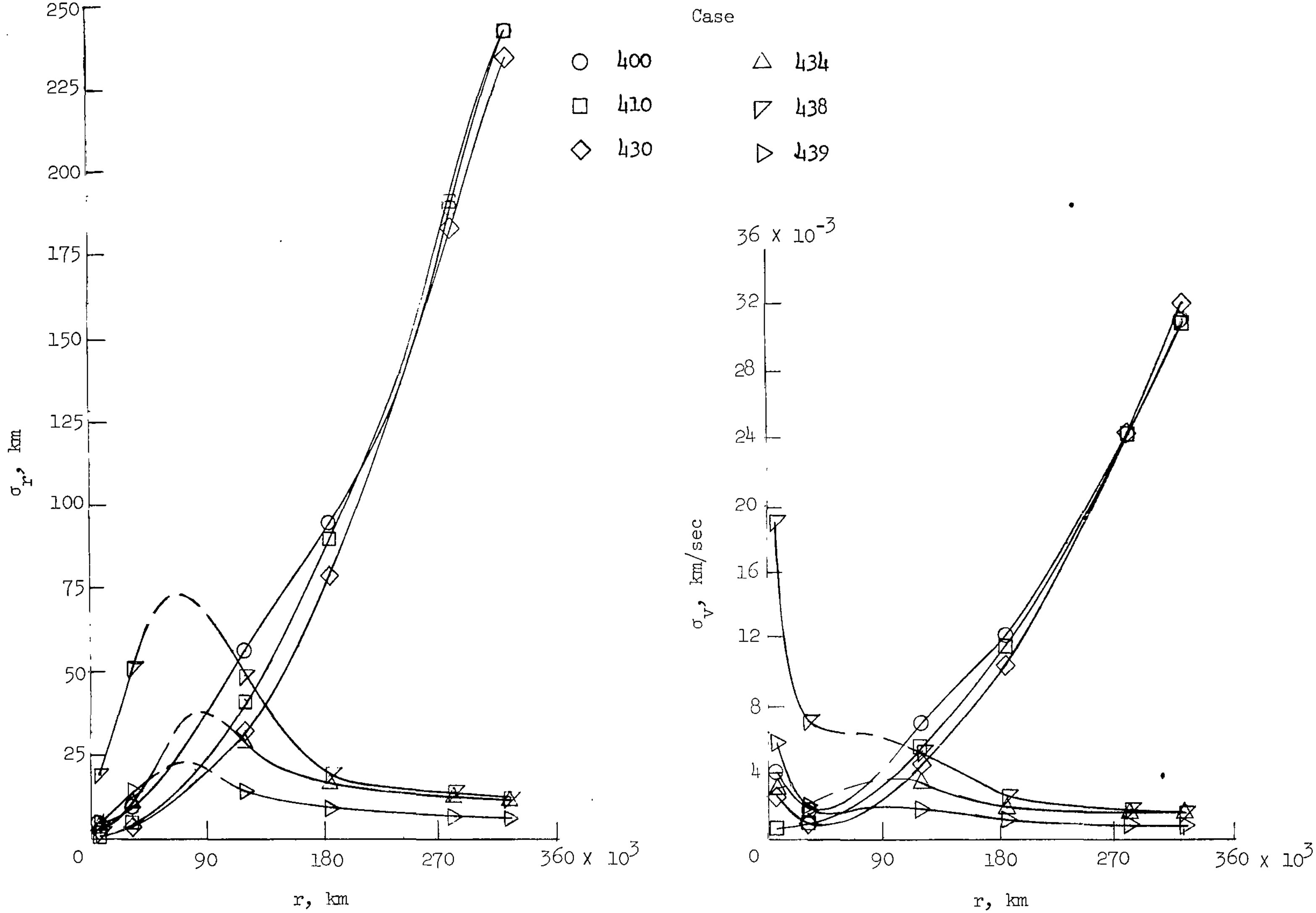

(a) Position.

(b) Velocity.

Figure 7.- Root sum square of standard deviations of errors in position and velocity as a function of the distance from the earth's center for some of the better cases involving observations of the stars and the earth or moon. Dashed portions of curves indicate uncertain regions.

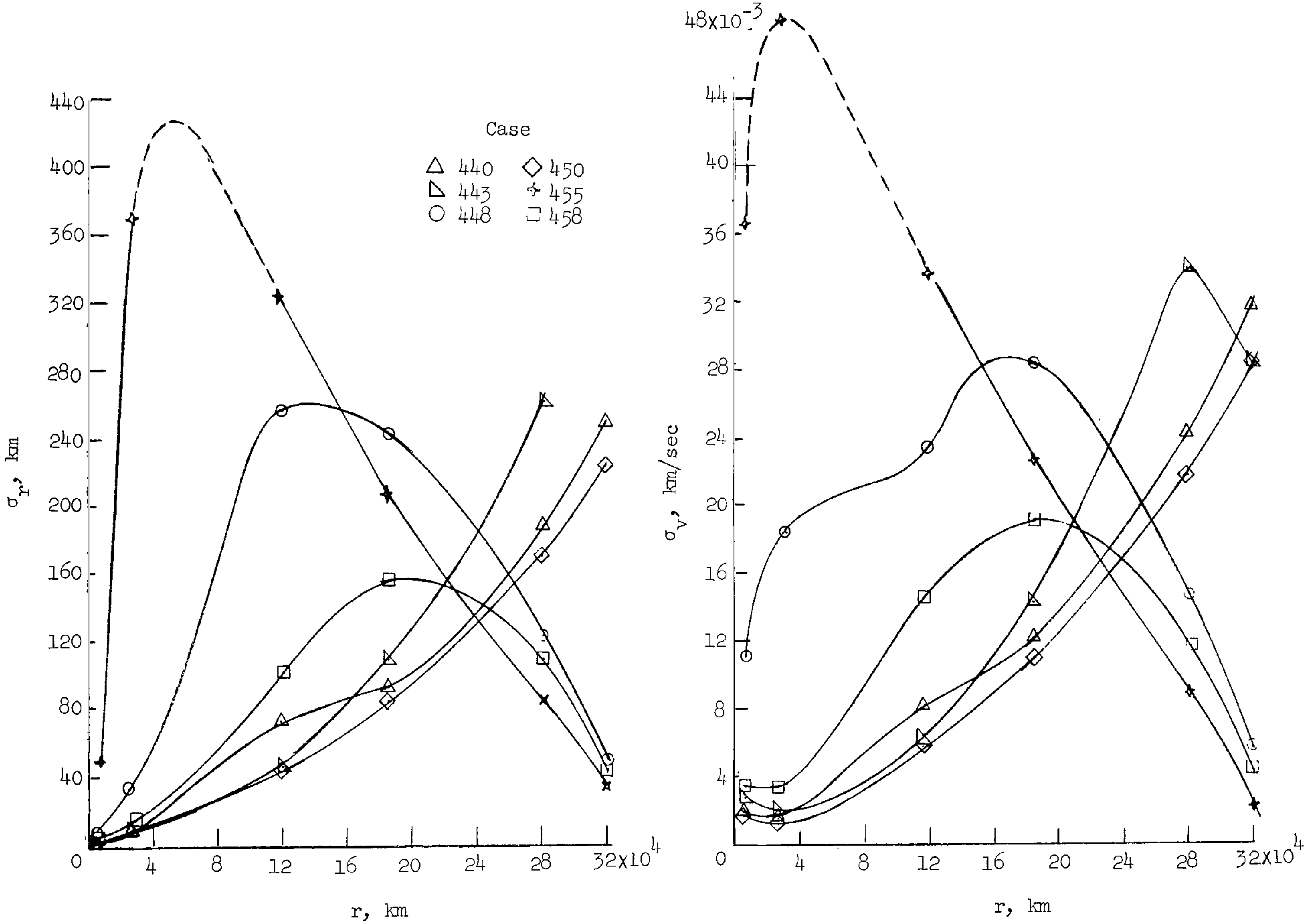

(a) Position.

(b) Velocity.

Figure 8.- Root sum square of standard deviations of errors in position and velocity as a function of the distance from the earth's center for some of the better cases involving landmarks and orbiting beacons of the earth or moon. Dashed portions of curves indicate uncertain regions.

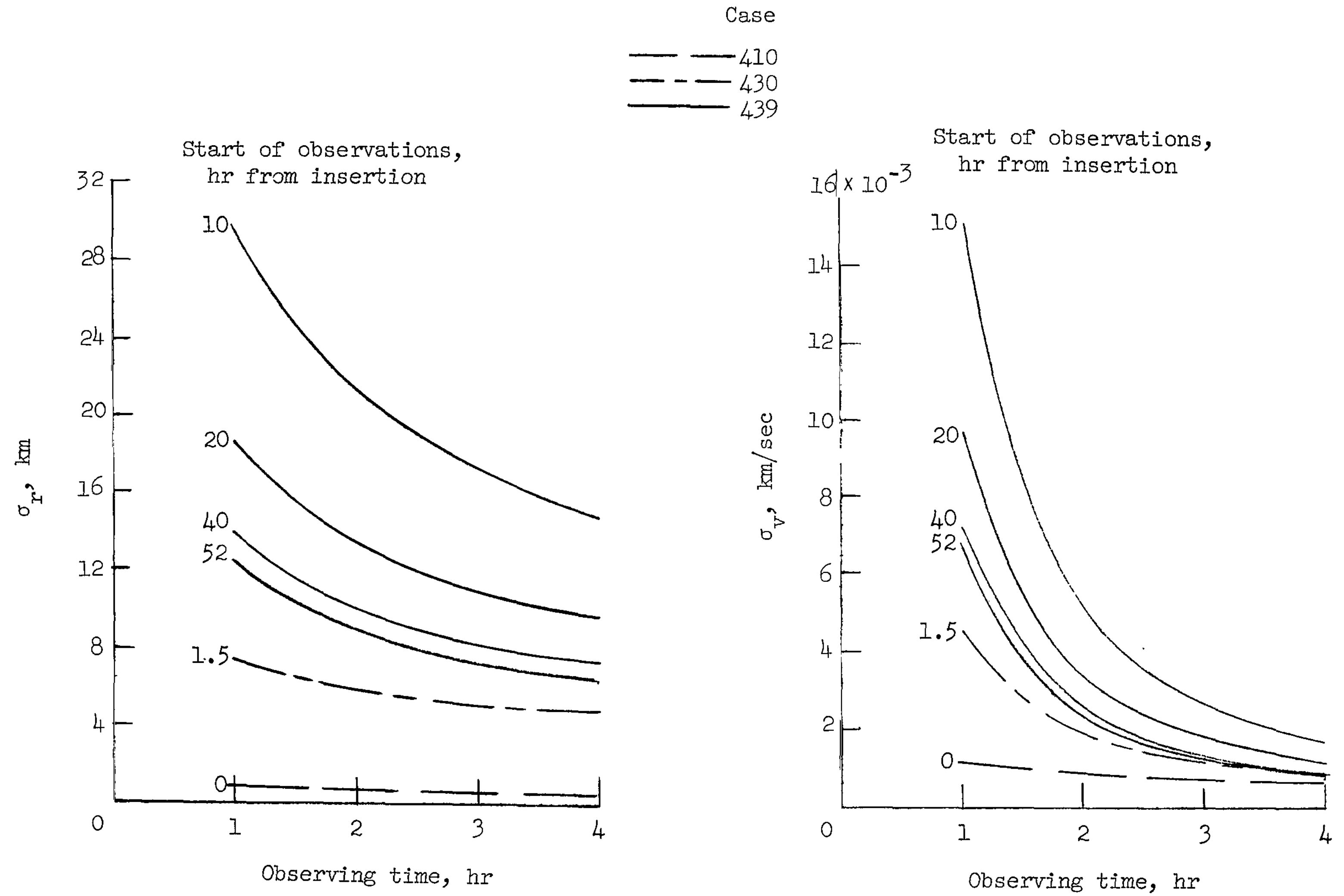

(a) Position.

(b) Velocity.

Figure 9.- Root sum square of standard deviations of errors in position and velocity for the best combination investigated in each observation region as a function of the observing time.

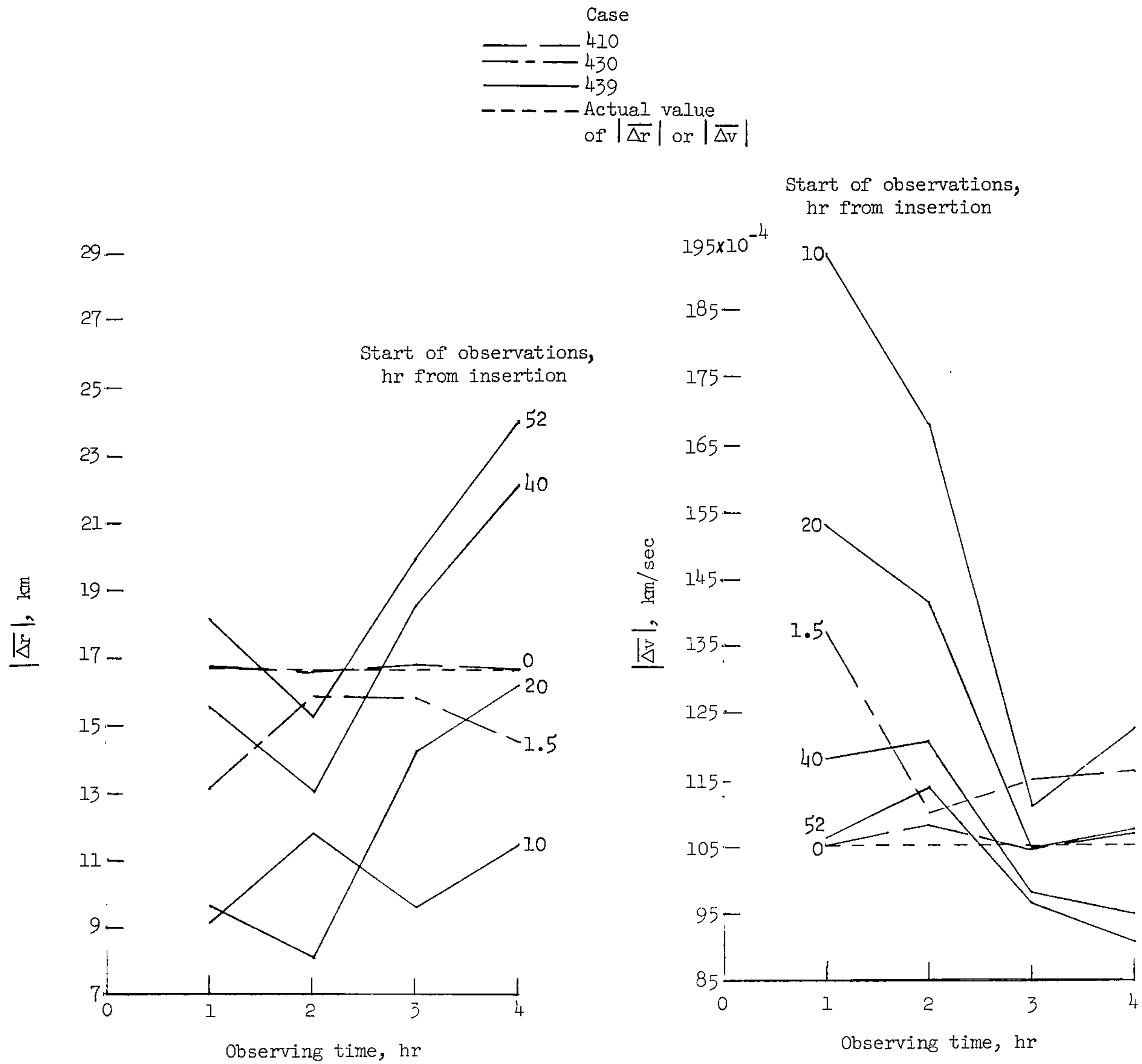

(a) Position.

(b) Velocity.

Figure 10.- Root sum square of best estimates of errors in position and velocity for the best combination investigated in each observation region as a function of the observing time.

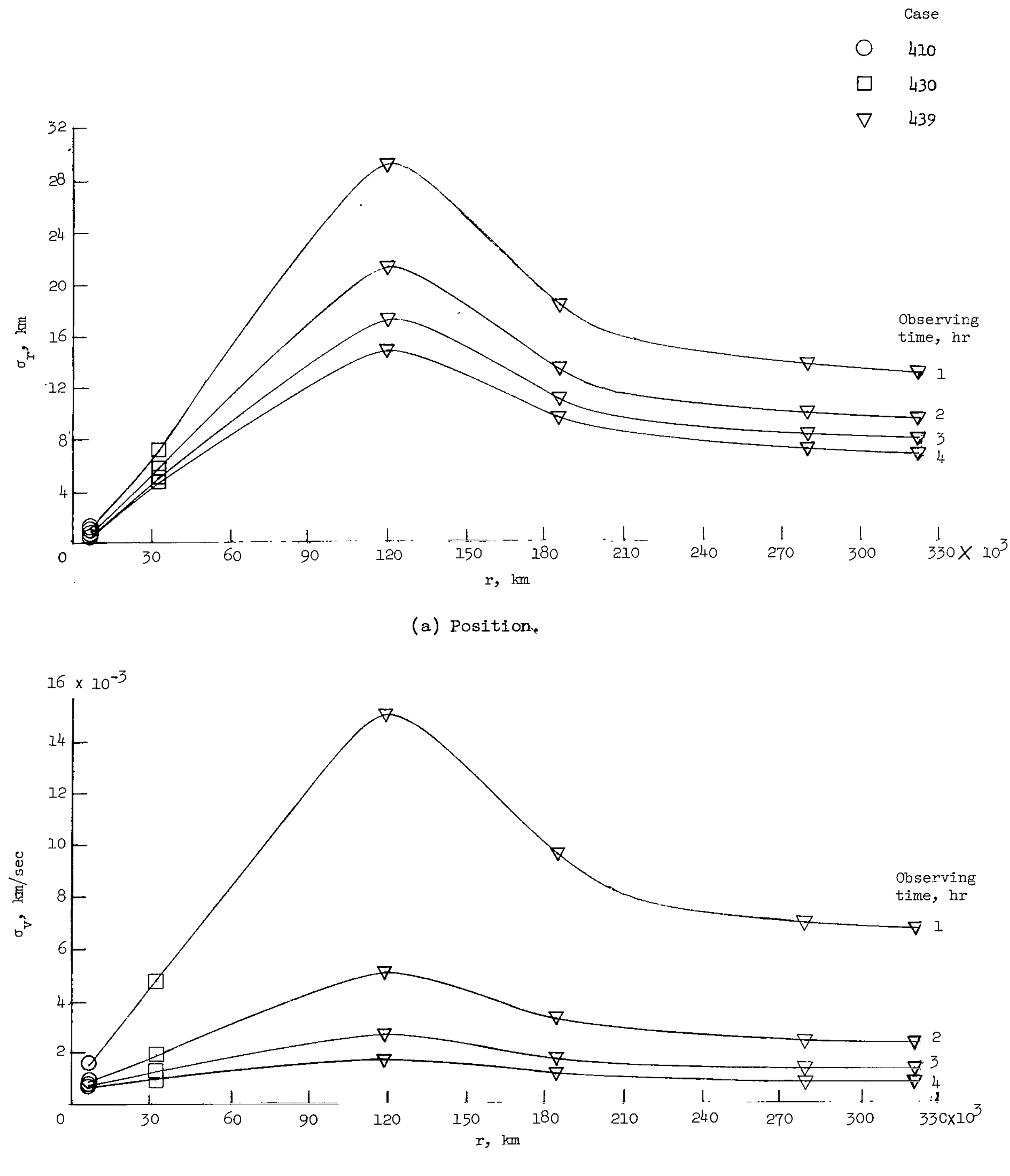

(a) Position.

(b) Velocity.

Figure 11.- Root sum square of the standard deviations of errors in position and velocity for the best combinations investigated over the earth-moon distance.

NASA-Langley, 1964 L-3666

2171? 5

"The aeronautical and space activities of the United States shall be conducted so as to contribute . . . to the expansion of human knowledge of phenomena in the atmosphere and space. The Administration shall provide for the widest practicable and appropriate dissemination of information concerning its activities and the results thereof."

—NATIONAL AERONAUTICS AND SPACE ACT OF 1958

NASA SCIENTIFIC AND TECHNICAL PUBLICATIONS

TECHNICAL REPORTS: Scientific and technical information considered important, complete, and a lasting contribution to existing knowledge.

TECHNICAL NOTES: Information less broad in scope but nevertheless of importance as a contribution to existing knowledge.

TECHNICAL MEMORANDUMS: Information receiving limited distribution because of preliminary data, security classification, or other reasons.

CONTRACTOR REPORTS: Technical information generated in connection with a NASA contract or grant and released under NASA auspices.

TECHNICAL TRANSLATIONS: Information published in a foreign language considered to merit NASA distribution in English.

TECHNICAL REPRINTS: Information derived from NASA activities and initially published in the form of journal articles.

SPECIAL PUBLICATIONS: Information derived from or of value to NASA activities but not necessarily reporting the results of individual NASA-programmed scientific efforts. Publications include conference proceedings, monographs, data compilations, handbooks, sourcebooks, and special bibliographies.

Details on the availability of these publications may be obtained from:

SCIENTIFIC AND TECHNICAL INFORMATION DIVISION

NATIONAL AERONAUTICS AND SPACE ADMINISTRATION

Washington, D.C. 20546